

Natural variations of maize ZmLecRK1 determine its interaction with ZmBAK1 and resistance patterns to multiple pathogens

Zhenju Li^{1,6}, Junbin Chen^{1,6}, Chuang Liu^{1,6}, Shengfeng He¹, Mingyu Wang^{1,2}, Lei Wang³, Vijai Bhaduria⁴, Shiwei Wang⁴, Wenyu Cheng¹, Hui Liu¹, Xiaohong Yang⁵, Mingliang Xu⁵, You-Liang Peng⁴ and Wangsheng Zhu^{1,*}

¹State Key Laboratory of Maize Bio-breeding/College of Plant Protection/Ministry of Agriculture and Rural Affairs Key Laboratory of Surveillance and Management for Plant Quarantine Pests, China Agricultural University, Beijing 100193, P.R. China

²Institute of Plant Protection and Microbiology, Zhejiang Academy of Agricultural Sciences, Zhejiang 310021, P.R. China

³Yazhouwan National Laboratory, Sanya, Hainan 572024, P.R. China

⁴Ministry of Agriculture and Rural Affairs Key Laboratory for Crop Pest Monitoring and Green Control, College of Plant Protection, China Agricultural University, Beijing 100193, P.R. China

⁵State Key Laboratory of Plant Environmental Resilience, College of Agronomy and Biotechnology, National Maize Improvement Center, Center for Crop Functional Genomics and Molecular Breeding, China Agricultural University, Beijing 100193, P.R. China

⁶These authors contributed equally to this article.

*Correspondence: Wangsheng Zhu (wangshengzhu@cau.edu.cn)

<https://doi.org/10.1016/j.molp.2024.09.006>

ABSTRACT

Maize (*Zea mays*) is one of the most important crops in the world, but its yield and quality are seriously affected by diverse diseases. Identifying broad-spectrum resistance genes is crucial for developing effective strategies to control the disease in maize. In a genome-wide study in maize, we identified a G-type lectin receptor kinase ZmLecRK1, as a new resistance protein against *Pythium aphanidermatum*, one of the causal pathogens of stalk rot in maize. Genetic analysis showed that the specific ZmLecRK1 allele can confer resistance to multiple pathogens in maize. The cell death and disease resistance phenotype mediated by the resistant variant of ZmLecRK1 requires the co-receptor ZmBAK1. A naturally occurring A404S variant in the extracellular domain of ZmLecRK1 determines the ZmLecRK1-ZmBAK1 interaction and the formation of ZmLecRK1-related protein complexes. Interestingly, the ZmLecRK1 susceptible variant was found to possess the amino acid S404 that is present in the ancestral variants of ZmLecRK1 and conserved among the majority of grass species, while the resistance variant of ZmLecRK1 with A404 is only present in a few maize inbred lines. Substitution of S by A at position 404 in ZmLecRK1-like proteins of sorghum and rice greatly enhances their ability to induce cell death. Further transcriptomic analysis reveals that ZmLecRK1 likely regulates gene expression related to the pathways in cell wall organization or biogenesis in response to pathogen infection. Taken together, these results suggest that the ZmLecRK1 resistance variant enhances its binding affinity to the co-receptor ZmBAK1, thereby enhancing the formation of active complexes for defense in maize. Our work highlights the biotechnological potential for generating disease-resistant crops by precisely modulating the activity of ZmLecRK1 and its homologs through targeted base editing.

Key words: natural variation, G-type lectin receptor-like kinase, co-receptor BAK1, broad-spectrum resistance, genome-wide association study, maize

Li Z., Chen J., Liu C., He S., Wang M., Wang L., Bhaduria V., Wang S., Cheng W., Liu H., Yang X., Xu M., Peng Y.-L., and Zhu W. (2024). Natural variations of maize ZmLecRK1 determine its interaction with ZmBAK1 and resistance patterns to multiple pathogens. *Mol. Plant.* **17**, 1606–1623.

INTRODUCTION

Plants are constantly exposed to various pathogens. To combat pathogen challenges, plants have evolved a two-tiered innate immune system, of which the first layer is mediated by plasma membrane-located pattern recognition receptors (PRRs) to detect pathogens and mount immune responses (Jones and Dangl, 2006). PRRs perceive and recognize pathogen-associated molecular patterns (PAMPs) or damage-associated molecular patterns (DAMPs) from the host, leading to pattern-triggered immunity (PTI) (Zipfel, 2014; Couto and Zipfel, 2016). PRRs include receptor-like kinases (RLKs) with functional intracellular kinase domains and receptor-like proteins (RLPs) lacking obvious intracellular signaling domains (Couto and Zipfel, 2016).

The first RLK ZmPK1 in plants was identified in maize (Walker and Zhang, 1990), and, subsequently, many RLKs have been characterized in plants (Yin et al., 2024). Among these RLKs, the G-type lectin receptor kinases (LecRKs) are notable for containing the D-mannose-binding lectin domain, S-locus glycoprotein domain, and plasminogen-apple-nematode (PAN) domain at the extracellular region. G-type RLKs play diverse roles in plants, such as regulating development and responses to environmental stimuli (Vaid et al., 2013). In *Arabidopsis thaliana*, the G-type LecRK AtRDA2 (resistant to DFPM inhibition of ABA signaling 2) and AtLORE (lipooligosaccharide-specific reduced elicitation) recognize the pathogen-derived sphingolipids and the medium-chain 3-hydroxy fatty acids (Kutschera et al., 2019; Luo et al., 2020; Schellenberger et al., 2021; Kato et al., 2022), respectively. In crops, G-type LecRK-encoding genes, such as *Pi-d2*, *SDS2*, and *OsLecRK1-3* in rice, and *SpSRLK-5* in tomato, were identified as quantitative resistance genes for either pathogens or insects (Chen et al., 2006; Catanzariti et al., 2015; Liu et al., 2015; Fan et al., 2018; Dai et al., 2023). In addition, many other G-type LecRKs have been characterized as regulators of symbiosis or responses to abiotic stress (Walker and Zhang, 1990; Tobias et al., 1992; Tobias and Nasrallah, 1996; Gilardoni et al., 2011; Sun et al., 2013a; Chen et al., 2013; Cheng et al., 2013; Trontin et al., 2014; Zou et al., 2015; Schnepf et al., 2018; Labbé et al., 2019; Park et al., 2019; Jinjun et al., 2020; Pan et al., 2020; Liu et al., 2021; Mondal et al., 2021; Qiao et al., 2021; Wang et al., 2023b; De et al., 2023; Shrestha et al., 2023; Zhou et al., 2023).

Upon recognizing the ligands derived from either pathogens or damaged plants, many PRRs form receptor complexes with co-receptors to activate downstream immune signaling in plants (Ma et al., 2016; DeFalco and Zipfel, 2021; Ngou et al., 2024). For example, in *Arabidopsis*, the LRR-RLK FLAGELLIN SENSING 2 (FLS2) activates immune response by forming receptor complex with the co-receptor BRI1-ASSOCIATED RECEPTOR KINASE 1 (BAK1) (Gómez-Gómez and Boller, 2000; Chinchilla et al., 2006, 2007; Roux et al., 2011) upon recognizing the bacterial flagellin epitope flg22 (Boller and Felix, 2009; Sun et al., 2013b; Robatzek and Wirthmueller, 2013; Couto and Zipfel, 2016). To date, only a few G-type LecRKs have been studied with detailed mechanisms. In *Brassica rapa*, the stigma-expressed G-type LecRK senses the pollen-derived peptide ligands S-LOCUS CYSTEIN-RICH PEPTIDES (SCRs) and induces reactive oxygen species (ROS) burst to prevent self-pollination (Takayama et al., 2001; Ivanov et al., 2010; Jany et al., 2019; Huang et al., 2023). In *Arabidopsis*, LORE forms

a homodimer to initiate immune signaling upon recognizing bacterial medium-chain 3-hydroxy fatty acids (Eschrig et al., 2024). LORE initiates xylem immunity against bacterial wilt disease, with its dephosphorylation by protein phosphatase LORE-associated protein phosphatase functioning as a surveillance system to balance immune signaling (Wang et al., 2023b). In rice, SPL11 CELL-DEATH SUPPRESSOR 2 (SDS2), a monocot-specific G-type LecRK lacking the PAN domain, phosphorylates receptor-like cytoplasmic kinases to activate downstream immune responses (Fan et al., 2018). However, the characterization of many G-type LecRKs, the requirement for co-receptors in G-type LecRK-mediated immunity, and the mechanisms by which they form immune complexes for downstream signaling remain unclear.

Maize (*Zea mays*) is one of the most important crops in the world, but its yield and quality are seriously affected by diverse diseases, including stalk rot (causal agent *Pythium* and *Fusarium*), banded leaf and sheath blight (causal agent *Rhizoctonia solani*), and southern leaf blight (causal agent *Bipolaris maydis*) (Balint-Kurti and Johal, 2009; Zhu et al., 2021). *Pythium* stalk rot is a soilborne disease primarily caused by *Pythium* spp., among which *P. aphanidermatum* can cause root rot, seedling blight, and stem rot (Wang and Duan, 2020). Utilizing resistant cultivars is one of the most economical and environmentally friendly measures to control plant diseases (Yang et al., 2017a; Zhu et al., 2021; Gou et al., 2023). Natural genetic variations are invaluable resources for identifying such disease-resistance genes in crops, particularly maize. Among reported disease-resistance genes in maize, several encode PRRs, including *ZmWAK*, *ZmWAK-RLK1*, *ZmWAKL*, and *ZmChSK1* (Hurni et al., 2015; Zuo et al., 2015; Yang et al., 2019; Chen et al., 2023a; Gou et al., 2023; Zhong et al., 2024). Although the maize genome encodes 79 G-type LecRK members, their roles as potential disease-resistance proteins in maize remain to be characterized.

Here, we report the isolation and functional characterization of a natural *ZmLecRK1* allele encoding G-type LecRK that confers resistance to multiple pathogens in maize. *ZmLecRK1* interacts with the leucine-rich repeat kinase ZmBAK1 to stimulate an immune response. We demonstrated that a natural A404S variant in the PAN domain of *ZmLecRK1* is the major causal polymorphism that determines the ability of *ZmLecRK1* to interact with ZmBAK1 and to form *ZmLecRK1*-related protein complexes.

RESULTS

ZmLecRK1 is significantly associated with multi-pathogen resistance in maize

Our previous genome-wide association study identified two chromosomal regions, including the distal of chromosome 1 and the top of chromosome 5, associated with resistance to *Pythium* stalk rot in maize (Liu et al., 2024). The significant single-nucleotide polymorphisms (SNPs) on chromosome 5 are located within the gene body of a single gene, *GRMZM2G330751*, predicted to encode a G-type lectin receptor kinase. We, therefore, named this gene *ZmLecRK1*. Four SNPs located in the first exon region of *ZmLecRK1* altered the amino acid sequence and were in strong linkage disequilibrium (LD) with the lead SNP 851 (Figure 1A and Supplemental Figure 1A), dividing the mapping population into

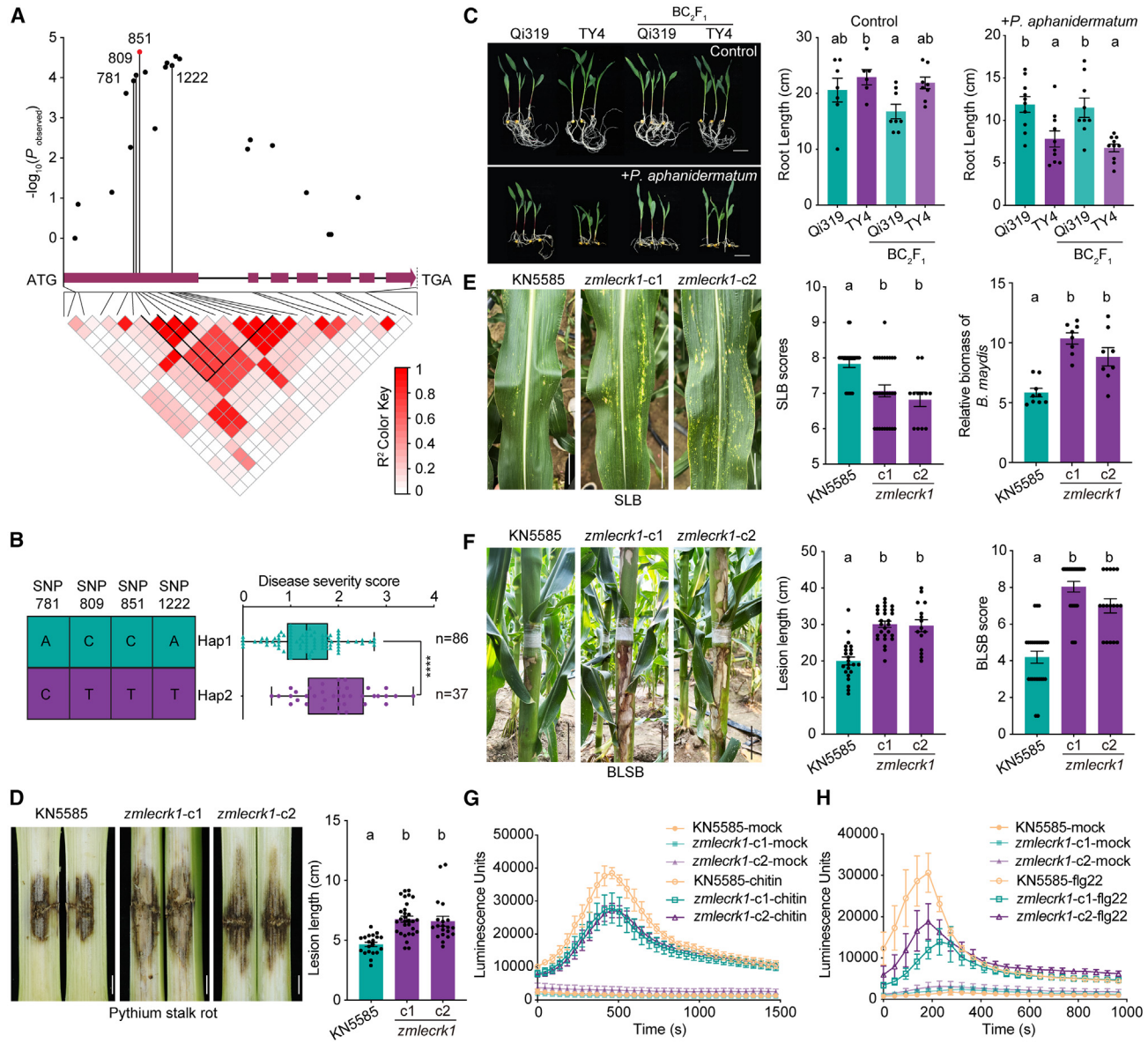


Figure 1. *ZmLecRK1* contributes to multi-pathogen resistance in maize.

(A) Genome-wide association hits at *ZmLecRK1* and pattern of local linkage disequilibrium (LD). The SNPs showing strong LD with the lead SNP are connected to the pairwise LD diagram with solid lines and highlighted with black lines.

(B) Haplotypes (Hap) of *ZmLecRK1* among maize inbred lines. *n* denotes the number of genotypes belonging to each haplotype group. (*****p* < 0.0001, Student's *t*-test).

(C) Representative seedling phenotype (left) and quantitative measurement of root length (middle and right) of Qi319, TY4, and BC₂F₁ population infected with *P. aphanidermatum* at 7 days post inoculation, non-infected plants as the control. Scale bars, 5 cm.

(D) Representative disease phenotype (left) and lesion length (right) of *zmlleckr1* lines and KN5585 infected with *P. aphanidermatum* at 21 days post inoculation in the field. Scale bars, 1 cm.

(E) Representative disease phenotype (left), southern leaf blight (SLB) score (middle), and relative biomass of *B. maydis* (right) of infected leaves of *zmlleckr1* lines and KN5585 at 21 days post inoculation in the field. Scale bars, 5 cm.

(F) Representative disease phenotype (left), lesion length (middle), and banded leaf and sheath blight (BLSB) score (right) of *zmlleckr1* lines and KN5585 infected with *R. solani* at 14 days post inoculation in the field. Scale bars, 5 cm.

(G and H) (G) Chitin- and (H) flg22-induced reactive oxygen species (ROS) production in KN5585 and *zmlleckr1* lines (mean ± SEM; *n* = 8). Letters indicate significantly different groups, as determined by one-way ANOVA followed by Tukey's test at $\alpha = 0.05$ (C–H).

two major haplotype groups, with 86 belonging to the resistant haplotype (Hap1, with mean a disease severity score [DSS] of 1.3) and 37 to the susceptible haplotype (Hap2, with a mean DSS of 2.0) (Figure 1B). To further verify the role of *ZmLecRK1*

in resistance to *P. aphanidermatum*, we examined the co-segregation of the *ZmLecRK1* genotype with the disease phenotype in the BC₂F₁ population derived from Qi319 (representative of the Hap1 resistance allele *ZmLecRK1*^{Qi319}) and TY4

(representative of the Hap2 susceptible allele *ZmLecRK1*^{TY4}). The root-tip disease phenotype of the *ZmLecRK1*^{Qi319} allele (with a mean DSS of 1.0) significantly differs from that of the *ZmLecRK1*^{TY4} allele (with a mean DSS of 2.3) (Supplemental Figure 1B). Indoor pot infection showed that the plants with *ZmLecRK1*^{Qi319} are more resistant to *P. aphanidermatum* than the plants with *ZmLecRK1*^{TY4}, showing longer roots after pathogen treatment (Figure 1C). Finally, we generated two *ZmLecRK1* knockout mutants in maize inbred line KN5585, which carries the resistant *ZmLecRK1*^{Qi319}-type allele, using the CRISPR-Cas9 gene-editing tool (Supplemental Figure 1C). Root and indoor pot infection assays also showed that the two *zmlecrk1* lines were more susceptible to *P. aphanidermatum* than KN5585 (Supplemental Figure 1D and 1E). Field trials further confirmed that the two *zmlecrk1* lines exhibited longer lesions following the *P. aphanidermatum* infection compared with KN5585 (Figure 1D). These results suggest that *ZmLecRK1* is a strong candidate gene for Pythium stalk rot resistance.

We also investigated whether *ZmLecRK1* contributes to resistance against other pathogens in maize. To this end, we compared the disease symptoms between KN5585 and the two *zmlecrk1* lines following infections with *R. solani*, *B. maydis*, and *Fusarium graminearum*, three major fungal pathogens affecting maize. The infection assay showed that the two *zmlecrk1* lines displayed increased susceptibility to *B. maydis* (Figure 1E) and *R. solani* (Figure 1F and Supplemental Figure 1F), but not to *F. graminearum* (Supplemental Figure 1G) in the field. Similar results were observed in greenhouse infection assays (Supplemental Figure 1H and 1I). It is plausible that the *ZmLecRK1*-mediated resistance has been overcome by *F. graminearum* through other mechanisms. Overall, these findings underscore the role of *ZmLecRK1* in conferring quantitative resistance to multiple pathogens in maize.

ROS-mediated defense against pathogens is an essential arm of PRR-regulated plant immunity (Zhou and Zhang, 2020). To explore the potential role of *ZmLecRK1* in ROS regulation, we examined its effects on ROS burst induction in response to chitin, a typical fungal PAMP. The result showed that ROS accumulation is significantly increased from 1 to 8 min after chitin treatment in KN5585; however, both *zmlecrk1* lines exhibited reduced ROS production in response to chitin (Figure 1G). We also assessed ROS accumulation following treatment with flg22, a typical bacterial PAMP. Consistent with the chitin-induced ROS assay, the *zmlecrk1* mutation significantly suppressed flg22-induced ROS accumulation (Figure 1H), suggesting that *ZmLecRK1* may be involved in enhancing immune responses triggered by diverse PAMPs, thereby conferring multiple disease resistance.

***ZmLecRK1*^{Qi319}, but not *ZmLecRK1*^{TY4}, induces cell death in *Nicotiana*, *Arabidopsis*, and maize**

To elucidate the distinctions between *ZmLecRK1*^{Qi319} and *ZmLecRK1*^{TY4}, we initially assessed the gene expression of both alleles in response to *P. aphanidermatum* infection. The qPCR assay showed that both alleles respond to *P. aphanidermatum* similarly (Figure 2A), indicating that expression differences were not the likely cause for resistance. Subsequent Sanger sequencing of the full-length *ZmLecRK1* genomic fragment from Qi319 and TY4 re-

vealed that the amino acid differences between *ZmLecRK1*^{Qi319} and *ZmLecRK1*^{TY4} are exclusively within the extracellular domain (ECD) (Figure 2B). Therefore, we reasoned that *ZmLecRK1*^{Qi319} and *ZmLecRK1*^{TY4} might differ in protein function. To investigate this hypothesis, we transiently expressed the resistance allele *ZmLecRK1*^{Qi319} in *Nicotiana benthamiana* leaves. Expression of the resistance *ZmLecRK1*^{Qi319} allele induced conspicuous cell death, whereas the susceptible *ZmLecRK1*^{TY4} allele did not trigger macroscopic cell death (Figure 2C and Supplemental Figure 2A). Correspondingly, overexpression of *ZmLecRK1*^{Qi319} but not *ZmLecRK1*^{TY4} in *A. thaliana* led to classical autoimmune phenotypes characterized by stunted plant growth and elevated expression of the defense marker gene *PR1* (Figure 2D and Supplemental Figure 2B). Finally, we assessed the ability of *ZmLecRK1*^{Qi319} and *ZmLecRK1*^{TY4} to induce cell death in maize protoplasts using luciferase reporter activity as an indicator of cell survival. Our results demonstrated that only *ZmLecRK1*^{Qi319} induced cell death, while *ZmLecRK1*^{TY4} did not (Figure 2E and Supplemental Figure 2C). Collectively, these findings demonstrate the functional distinction between *ZmLecRK1*^{Qi319} and *ZmLecRK1*^{TY4} in inducing cell death across different plant species.

To further understand the function of *ZmLecRK1*, we generated the *ZmLecRK1*-Venus fusion protein to examine their subcellular localization. Both *ZmLecRK1*^{Qi319}-Venus and *ZmLecRK1*^{TY4}-Venus fusion proteins are co-localized with the membrane-impermeable dye FM4-64 in the maize protoplasts, indicating their association at the plasma membrane as membrane proteins (Supplemental Figure 2D). Next, we investigated whether *ZmLecRK1* functions as a kinase protein. Given that *ZmLecRK1*^{Qi319} and *ZmLecRK1*^{TY4} share an identical kinase domain, *ZmLecRK1*-KD was used to describe the kinase domain of both variants. *In vitro* kinase activity assay showed that *ZmLecRK1*-KD can auto-phosphorylate, whereas the kinase-dead variant *ZmLecRK1*-KD^{K548R} cannot, confirming that *ZmLecRK1*-KD is a functional kinase (Figure 2F). Finally, we generated *ZmLecRK1* kinase-dead mutants by substituting the essential arginine-aspartate (RD) residues in the catalytic loop and conserved lysine residues in the ATP-binding pocket with arginine-aspartic (RN) and arginine residues. Cell-death assay showed that neither *ZmLecRK1*^{Qi319/D645N} nor *ZmLecRK1*^{Qi319/K548R} induces cell death in *N. benthamiana* leaves (Figure 2G and Supplemental Figure 2E). These results showed that kinase activity is required for *ZmLecRK1*^{Qi319}-induced cell death.

Finally, we found that *ZmLecRK1*^{Qi319}-induced cell death can be fully inhibited by treatment with the Ca²⁺ channel blocker LaCl₃ (Supplemental Figure 2F). Moreover, *ZmLecRK1*^{Qi319} still induces cell death in *N. benthamiana eds1-1* (enhanced disease susceptibility 1-1) mutant (Qi et al., 2018), suggesting that *ZmLecRK1*^{Qi319}-induced cell death is independent of EDS1, a conserved and essential component of nucleotide oligomerization domain-like receptor (NLR) protein-mediated cell death and disease resistance in plants (Supplemental Figure 2G and 2H).

***ZmLecRK1*-mediated cell death and disease resistance is *ZmBAK1*-dependent**

PRRs usually form dynamic complexes with regulatory receptor kinases at the plasma membrane to activate immune signaling (Couto and Zipfel, 2016). To identify the potential components

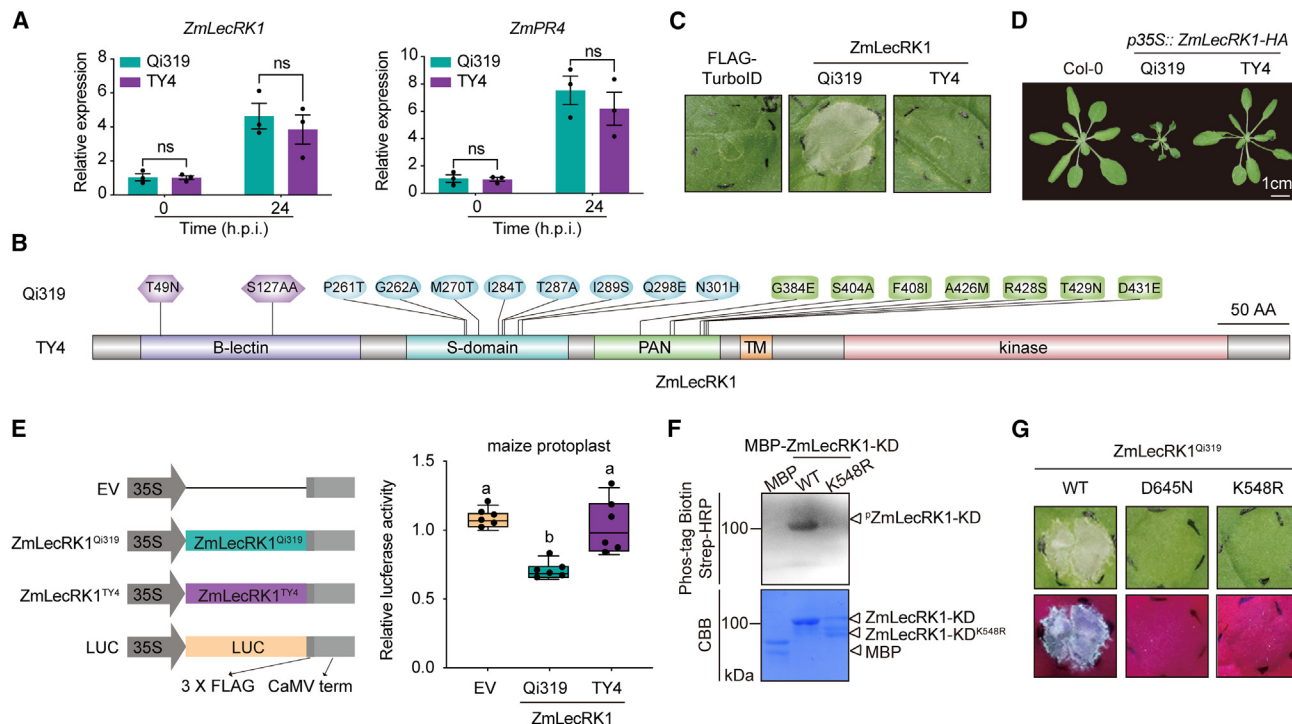


Figure 2. ZmLecRK1^{Qi319} but not ZmLecRK1^{TY4} induces cell death in *Nicotiana*, *Arabidopsis*, and maize.

(A) Gene expression of *ZmLecRK1* (left) and *ZmPR4* (right) in response to *P. aphanidermatum* infection from Qi319 and TY4 ($n = 3$ biological replicates; ns, not significant; Student's *t*-test).

(B) Natural variations between *ZmLecRK1*^{Qi319} and *ZmLecRK1*^{TY4}.

(C) Representative phenotype of *N. benthamiana* leaves expressing *ZmLecRK1*^{Qi319} and *ZmLecRK1*^{TY4}.

(D) Representative 4-week-old *Arabidopsis* T₃ transgenic plants with *p35S::ZmLecRK1*^{Qi319}-HA and *p35S::ZmLecRK1*^{TY4}-HA, grown at 23°C long day.

(E) Schematic diagrams (left) of constructs and phenotype (right) of maize protoplasts expressing *ZmLecRK1*^{Qi319} and *ZmLecRK1*^{TY4}. The LUC activity in maize protoplasts is co-transfected with different vector combinations. Empty vectors served as the negative control. Letters indicate significantly different groups, as determined by one-way ANOVA followed by Tukey's test at $\alpha = 0.05$.

(F) Kinase activity assay of *ZmLecRK1*-KD. The recombinant MBP-tagged *ZmLecRK1*-KD and its kinase site-mutated variants were subjected to kinase activity assays. The phosphorylated proteins were detected by Phos-tag biotin and streptavidin-HRP.

(G) Representative phenotype of *N. benthamiana* leaves expressing *ZmLecRK1*^{Qi319} and its kinase-dead variants. The leaves were photographed at 72 h post infiltration, and the lower one was photographed under UV.

associated with *ZmLecRK1*, we performed immunoprecipitation (IP) using the extract from maize protoplasts expressing *ZmLecRK1*-FLAG followed by mass spectrometry (MS), which identified a leucine-rich repeat kinase (GRMZM2G145720) as a *ZmLecRK1* interactor (Figure 3A; Supplemental Table 1). Homologs searching and phylogenetic analysis revealed that *GRMZM2G145720*-encoded leucine-rich repeat kinase is a homolog of the co-receptor kinase BAK1s in *Arabidopsis* (BAK1) and *N. benthamiana* (NbSERK3A and NbSERK3B). Additionally, the maize B73 reference genome encodes two other homologs of *GRMZM2G145720*, namely *GRMZM2G019317* and *GRMZM2G010693*, which cluster in the same clade with *AtBAK1*, *NbSERK3A*, and *NbSERK3B* (Supplemental Figure 3A). Although previous literature has reported a *ZmBAK1* (*GRMZM2G015933*) in maize (Cao et al., 2022), it is noteworthy that this variant lacks the essential kinase domain. We prefer to designate *GRMZM2G145720* as *ZmBAK1* according to the record in MaizeGDB (www.maizegdb.org).

Although BAK1 has been characterized as a co-receptor of many PPRs in *Arabidopsis* for immune signaling activation (Ma et al., 2016), it is unclear whether G-type LecRKs require BAK1 as

co-receptor for signal transduction. We wondered whether *ZmBAK1* acts as a co-receptor of *ZmLecRK1*. To test this assumption, we first asked whether the two NbBAK1s (*NbSERK3A* and *NbSERK3B*) are required for *ZmLecRK1*-induced cell death in *N. benthamiana*. To do so, we used the virus-induced gene silencing (VIGS) toolkit (Senthil-Kumar and Mysore, 2014) to silence *NbBAK1* and the RLP co-receptor encoding gene *NbSOBIR1* as a control in *N. benthamiana* (van der Burgh et al., 2019). The qPCR analysis showed that the relative expression levels of *NbBAK1* and *NbSOBIR1* were reduced by approximately 82% and 67%, respectively, compared to *TRV:GFP* control plants (Supplemental Figure 3B). *ZmLecRK1*^{Qi319} was then transiently expressed in the leaves of these two silenced plants, using BAX as a negative control and *Phytophthora infestans* PAMP INF1 as a positive control (Domazakis et al., 2018). The results showed that *ZmLecRK1*-induced cell death was dramatically suppressed in *NbBAK1*-silenced plants but not in *NbSOBIR1*-silenced plants (Figure 3B and Supplemental Figure 3C), supporting that the co-receptor NbBAK1 is required for *ZmLecRK1*-induced cell death in *N. benthamiana*. To ascertain whether *ZmBAK1* serves as a co-receptor of *ZmLecRK1* in maize, we generated *ZmBAK1* knockout mutants in the maize inbred line KN5585 harboring a resistant

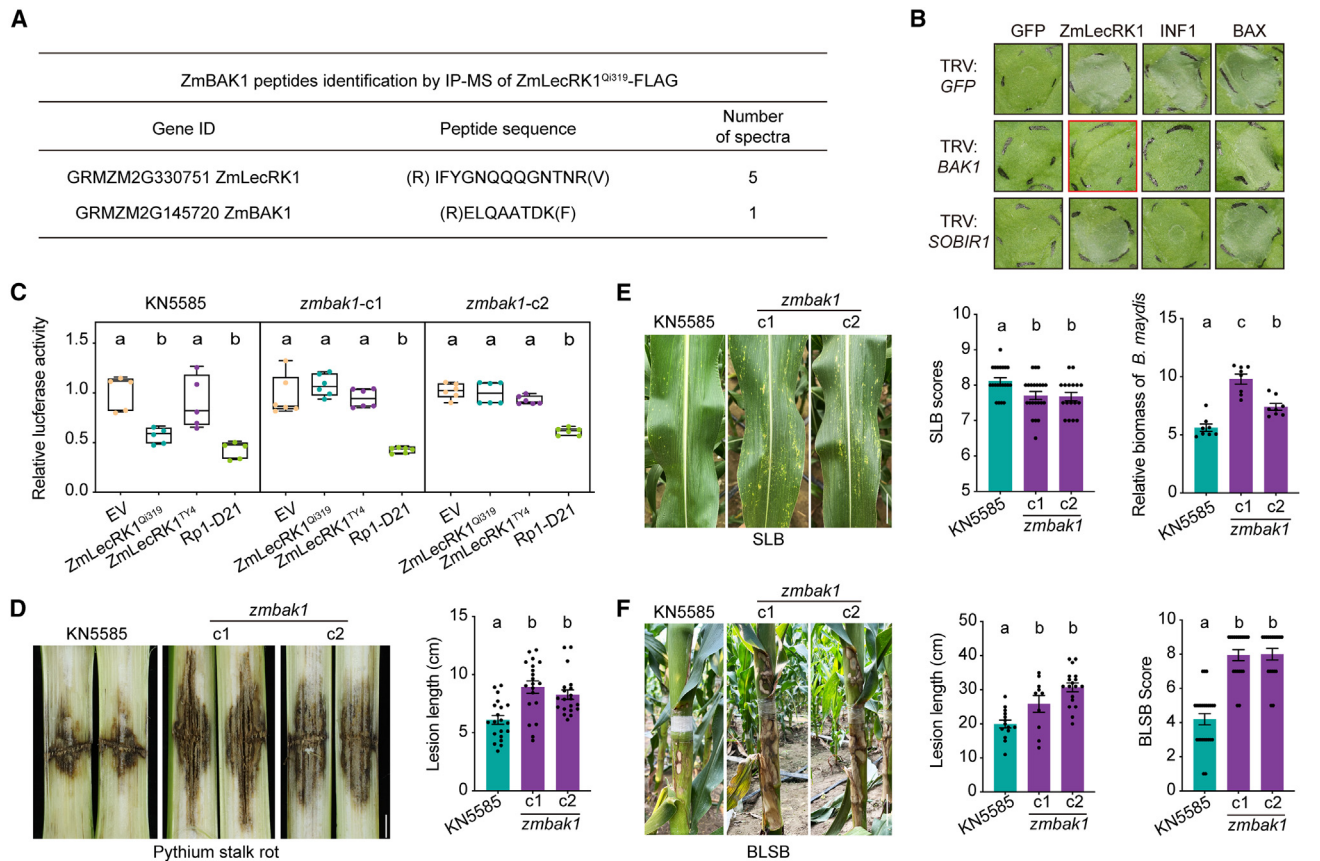


Figure 3. ZmBAK1 is required for ZmLecRK1-induced cell death and positively regulates multi-pathogen resistance.

(A) Identification of *ZmLecRK1*^{Qi319} and its interacting *ZmBAK1* by immunoprecipitation-MS analysis.

(B) Representative leaves show that *ZmLecRK1*^{Qi319}-induced cell death requires NbBAK1, not NbSOBIR1. GFP and INF1 were used as the negative and positive controls, respectively.

(C) *ZmLecRK1*^{Qi319}-triggered cell death in maize protoplasts from KN5585 and *zmbak1* lines. The LUC activity in different maize protoplasts is co-transfected with different vector combinations. Rp1-D21 and empty vector served as positive and negative controls, respectively.

(D) Representative disease phenotype in the field (left) and lesion length (right) of *zmbak1* lines and KN5585 infected with *P. aphanidermatum* at 21 days post inoculation. Scale bars, 1 cm.

(E) Representative disease phenotype in the field (left), SLB score (middle), and related biomass of *B. maydis* (right) of *zmbak1* lines and KN5585 infected with *B. maydis* at 21 days post inoculation. Scale bars, 5 cm.

(F) Representative disease phenotype in the field (left), lesion length (middle), and BLSB score (right) of *zmbak1* lines and KN5585 infected with *R. solani* at 14 days post inoculation. Scale bars, 5 cm. Letters indicate significantly different groups, as determined by one-way ANOVA followed by Tukey's test at $\alpha = 0.05$ (C-F).

ZmLecRK1^{Qi319}-type allele using the CRISPR-Cas9 gene-editing toolkit (Supplemental Figure 3D). Although *Arabidopsis bak1* mutants showed accelerated cell death (or tissue damage) (Kemmerling et al., 2007), neither of two *zmbak1* lines display this phenotype. We also measured the growth phenotype of the *zmbak1* lines, and found that the plant height of *zmbak1*-c1, with a mean height of 167.4 cm, is slightly shorter than KN5585, which has a mean height of 178.5 cm. Conversely, *zmbak1*-c2, with a mean height of 177.5 cm, did not show a significant difference from KN5585 at the V12 stage (Supplemental Figure 3E). These observations enable us to investigate the genetic dependence of *ZmLecRK1*-triggered cell death on *ZmBAK1*. As shown in Figure 3C, *ZmLecRK1*^{Qi319}-induced cell death was significantly suppressed in the protoplast generated from both the two *zmbak1* lines, while the NLR protein Rp1-D21-induced cell death was not affected (Chintamanani et al., 2010; Smith et al., 2010; Sun et al.,

2023). These results show that *ZmLecRK1*^{Qi319}-induced cell death is *ZmBAK1* dependent in maize.

To evaluate the involvement of *ZmBAK1* in the resistance of maize to *Pythium* stalk rot in maize, the two *zmbak1* lines were treated with *P. aphanidermatum*. In field trials, both *zmbak1* lines exhibited a longer lesion length than KN5585 carrying the *ZmLecRK1*^{Qi319}-type allele by infecting *P. aphanidermatum* (Figure 3D; Supplemental Table 2 and 3). Consequently, both mutant alleles had a higher disease index and shorter root length than the control line KN5585 in root and indoor pot infection assay (Supplemental Figure 3F and 3G). In addition, *zmbak1* mutants also show enhanced susceptibility to *B. maydis* (Figure 3E) and *R. solani* (Figure 3F) in the field. Together, these results suggest that *ZmBAK1* is required for *ZmLecRK1*-mediated resistance in maize.

Allelic variation in ZmLecRK1 affects its binding affinity to ZmBAK1

To understand the differential capability of the two ZmLecRK1 alleles in triggering cell death, we first examined the formation of high-order complexes by ZmLecRK1^{Qi319} and ZmLecRK1^{TY4} in plants. In the stable transgenic *Arabidopsis*, ZmLecRK1^{Qi319} was found in protein complexes exceeding 300 kDa as determined by blue native PAGE (BN-PAGE), whereas no significant signal was detected in the ZmLecRK1^{TY4} plants (Figure 4A). A similar pattern was also observed in maize protoplasts, forming complexes of above 300 kDa, in contrast to ZmLecRK1^{TY4}, which did not form such complexes (Figure 4B). Since ZmLecRK1^{Qi319} tends to form more robust complexes than ZmLecRK1^{TY4} *in planta*, we postulated that ZmLecRK1^{Qi319} interacts more strongly with ZmBAK1 compared to ZmLecRK1^{TY4}. This hypothesis was tested using Co-IP and split-luciferase complementation (SLC) assays, which indicated that full-length ZmBAK1 preferentially interacts with ZmLecRK1^{Qi319} over ZmLecRK1^{TY4} (Figure 4C and 4D and Supplemental Figure 4A). As ZmLecRK1^{Qi319} and ZmLecRK1^{TY4} differ only in ECD (Figure 2B), we investigated whether ZmLecRK1-ECD contributes to the observed differences in binding affinity with ZmBAK1. Both SLC and Co-IP assays indicated that ZmBAK1-ECD exhibited a higher affinity for ZmLecRK1^{Qi319}-ECD compared to ZmLecRK1^{TY4}-ECD (Figure 4E and 4F and Supplemental Figure 4B). Consistently, ZmBAK1-ECD was found to associate more with ZmLecRK1^{Qi319}-ECD than with ZmLecRK1^{TY4}-ECD in maize protoplast (Figure 4G).

Since PRRs may also form homodimers to amplify the downstream signaling (Macho and Zipfel, 2014), we further tested how ZmBAK1 affects the self-interaction of ZmLecRK1. The Co-IP and SLC assays showed that ZmBAK1 enhanced the self-interaction strength of ZmLecRK1^{Qi319} but not ZmLecRK1^{TY4} (Figure 4H and Supplemental Figure 4C and 4D). These results together show that ZmBAK1 interacts more robustly with ZmLecRK1^{Qi319} than ZmLecRK1^{TY4}, increasing the formation of more protein complexes.

Because ZmLecRK1^{Qi319} and ZmBAK1 both positively regulate resistance against *R. solani*, *B. maydis*, and *P. aphanidermatum*, we investigated whether these pathogens regulate PRR complex formation to enhance resistance. As anticipated, *P. aphanidermatum* treatment promoted the ZmLecRK1^{Qi319} association with the ZmBAK1 in *N. benthamiana*, as demonstrated by the SLC assays (Figure 4I and Supplemental Figure 4E). However, due to the inability of *R. solani* and *B. maydis* to infect *N. benthamiana*, we could not directly assess the effect of these two fungal pathogens on ZmLecRK1^{Qi319}-ZmBAK1 interaction *in vivo*. To address this, we tested this hypothesis using a typical fungal PAMP chitin, a known PAMP that elicits basal defense responses. The results showed that chitin treatment also enhances the interaction between ZmLecRK1^{Qi319} and ZmBAK1 (Figure 4J and Supplemental Figure 4F). Therefore, binding of ZmLecRK1 to ZmBAK1 occurs constitutively and is further enhanced in response to pathogens or PAMPs treatment.

A404 residue in the PAN domain is required for ZmLecRK1-triggered cell death

To identify the causative polymorphisms responsible for the differential functions of ZmLecRK1 in inducing cell death, we sequenced

the full-length ZmLecRK1 genomic fragment from Qi319 and TY4. Sequence alignment revealed that the amino acid differences between ZmLecRK1^{Qi319} and ZmLecRK1^{TY4} are exclusively found in the ECD (Figure 2B). We exchanged the B-lectin, S-locus, and PAN domains between ZmLecRK1^{Qi319} and ZmLecRK1^{TY4} for the cell-death assay. The results showed that the exchange of the PAN domain and S-locus domain, but not the B-lectin domain, activates cell death induced by ZmLecRK1^{TY4} and inactivates ZmLecRK1^{Qi319} (Figure 5A and 5B and Supplemental Figure 5A). This suggests that variations in the PAN and S-locus domains contribute to the differential capability of the two alleles to trigger cell death, with the PAN domain playing a major role. The PAN domain of ZmLecRK1^{Qi319} contains seven amino acids that differ from ZmLecRK1^{TY4} (Figure 2B). To identify the causative residues, we generated a series of constructs with mutations covering all differences between ZmLecRK1^{Qi319} and ZmLecRK1^{TY4}. We found that mutations E384G, I408F, and M426A/S428R/N429T/S431D have no impact on ZmLecRK1^{Qi319}-induced cell death in *N. benthamiana*, while mutation A404S drastically suppresses ZmLecRK1^{Qi319}-induced cell death (Figure 5C and Supplemental Figure 5B). In the context of ZmLecRK1^{TY4}, either the G384E or S404A mutation alone partially enhanced the cell death phenotype, while the other mutations had no obvious effects (Figure 5C and Supplemental Figure 5C). When both E384 and A404 were introduced in ZmLecRK1^{TY4}, the ZmLecRK1^{TY4} mutant greatly enhanced cell death (Figure 5C).

To further test the effects of the A404S mutation on the function of ZmLecRK1^{Qi319} in maize, we used luciferase reporter activity to monitor cell survival in maize protoplasts expressing different ZmLecRK1 alleles. As shown in Figure 5D, maize protoplasts expressing ZmLecRK1^{Qi319} with the A404S mutation showed a much lower frequency of cell death, as indicated by higher luciferase reporter activity, similar to ZmLecRK1^{TY4} and the empty vector. Conversely, ZmLecRK1^{TY4} with G384E and S404A mutations induced a higher frequency of cell death than wild-type ZmLecRK1^{TY4} in maize protoplast (Figure 5D). Taken together, these results show that A404 is one of the critical residues for ZmLecRK1-induced cell death.

To understand the genetic variation of the residue at position 404 in other G-type LecRKs, we first analyzed the sequences of all 69 G-type LecRKs harboring PAN domain from the maize B73 reference genome (<https://www.maizegdb.org/>). Serine at the 404 position was found in 10 out of 69 G-type LecRKs, while no alanine at this position was identified (Supplemental Figure 5D). We next examined the sequence diversity of the PAN domain in ZmLecRK1 orthologs from 85 maize inbred lines and 21 other grass species. Sequence alignment revealed that LecRKs with S404 are conserved in most grass species (26 of 40) (Supplemental Figure 5E), while LecRKs with A404 are only present in a few maize inbred lines (43 of 85) (Figure 5E; Supplemental Table 2 and 3). Moreover, the maize ancestor teosinte encodes a ZmLecRK1 ortholog (GenBank: JAOPSE010000017.1) with S404. These results suggest that ZmLecRK1^{TY4} with S404 is the ancestral allele, while ZmLecRK1^{Qi319} with A404 is likely newly evolved in maize. Interestingly, mutating corresponding S to A in the ZmLecRK1's homologs in sorghum (SbLecRK1, GenBank: KAG0548914.1, S395A) and rice (OsLecRK6, GenBank: LOC4337108, S379A) greatly enhanced their ability to induce cell death in *N. benthamiana* (Figure 5F and 5G and Supplemental Figure 5F and 5G). Consistently, the S379A

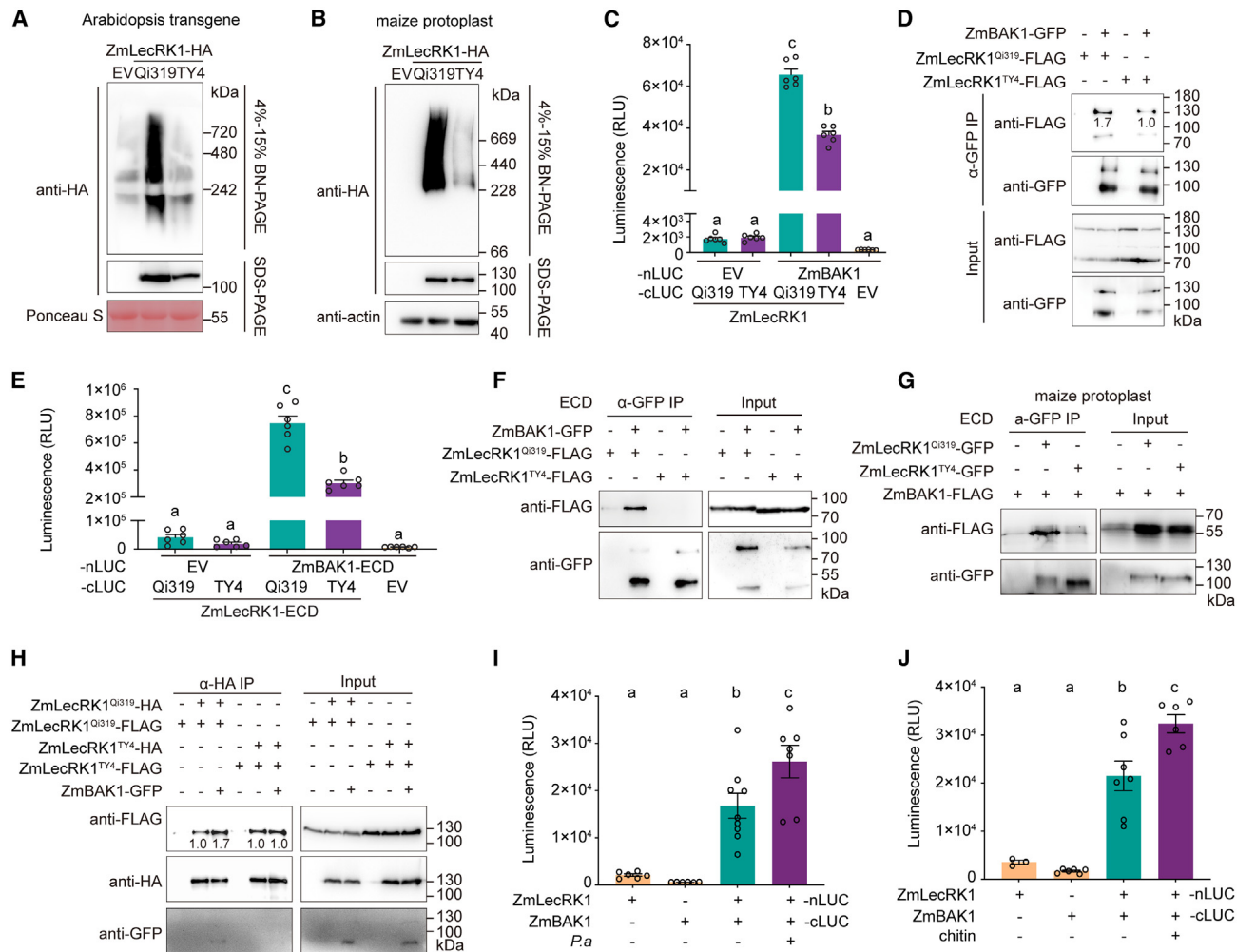


Figure 4. ZmLecRK1^{Qi319} interacts more robustly with ZmBAK1 than ZmLecRK1^{TY4} and forms more protein complexes.

(A and B) ZmLecRK1-associated complexes in ZmLecRK1-overexpressed *A. thaliana* (A) and maize protoplasts (B), as shown by BN-PAGE.

(C and D) The interaction between full-length ZmBAK1 and ZmLecRK1^{Qi319} is stronger than with ZmLecRK1^{TY4} by SLC (C) and coIP (D) assays in *N. benthamiana*.

(E) The comparison of interaction strength of ZmLecRK1^{Qi319}-ECD, and ZmLecRK1^{TY4}-ECD with ZmBAK1-ECD, as shown by SLC in *N. benthamiana*.

(F and G) Compared to ZmLecRK1^{TY4}-ECD, ZmLecRK1^{Qi319}-ECD interacts more strongly with ZmBAK1-ECD, as shown by coIP assay in *N. benthamiana* leaves (F) and maize protoplast (G).

(H) ZmBAK1 can specifically enhance the self-interaction strength of ZmLecRK1^{Qi319}, as shown by Co-IP in *N. benthamiana*. Numbers on gel blots indicate relative arbitrary densitometry units of corresponding bands after normalization to the sample without ZmBAK1-GFP in grouped samples.

(I and J) Effect of *P. aphanidermatum* (I) and chitin (J) on the ZmLecRK1^{Qi319}-ZmBAK1 interaction, as shown by SLC. Letters indicate significantly different groups, as determined by one-way ANOVA followed by Tukey's test at $\alpha = 0.05$ (C, E, I, and J).

mutation in OsLecRK6 significantly enhanced cell death in rice protoplasts (Figure 5H). We also examined the genetic diversity of S379 residue in OsLecRK6 from different rice varieties. Sequence alignment revealed that position 379 is exclusively conserved as the susceptible serine residue in the OsLecRK6 orthologs across all 264 rice varieties tested in this study (Supplemental Figure 5H; Supplemental Table 4). These results show that the newly evolved A404 residue is required for the function of ZmLecRK1 and its homologs in grass species.

A404S mutation impairs the ZmLecRK1^{Qi319}-ZmBAK1 interaction

To understand how the A404S mutation affects the interaction of ZmLecRK1^{Qi319} with ZmBAK1, we modeled the structure of the

ZmLecRK1^{Qi319}-PAN domain with ColabFold (Supplemental Figure 6A) (Mirdita et al., 2022). The structural analysis revealed that substituting A404 with S404 significantly altered the PAN domain conformation (Supplemental Figure 6B). AlphaFold2-multimer modeling of the ZmLecRK1^{Qi319}-ECD-ZmBAK1-ECD complex indicated that A404 in ZmLecRK1^{Qi319} is one of the critical residues for interacting with ZmBAK1 and that the A404S mutation in the ECD domain of ZmLecRK1^{Qi319} significantly weakens this interaction (Figure 6A). To experimentally validate the prediction, we first co-expressed ZmLecRK1-GFP and ZmLecRK1 mutation-GFP together with ZmBAK1-FLAG for Co-IP assays. The result showed that ZmLecRK1^{Qi319} with mutation A404S lost the ability to interact with ZmBAK1 (Figure 6B), which was corroborated by the SLC assay (Supplemental

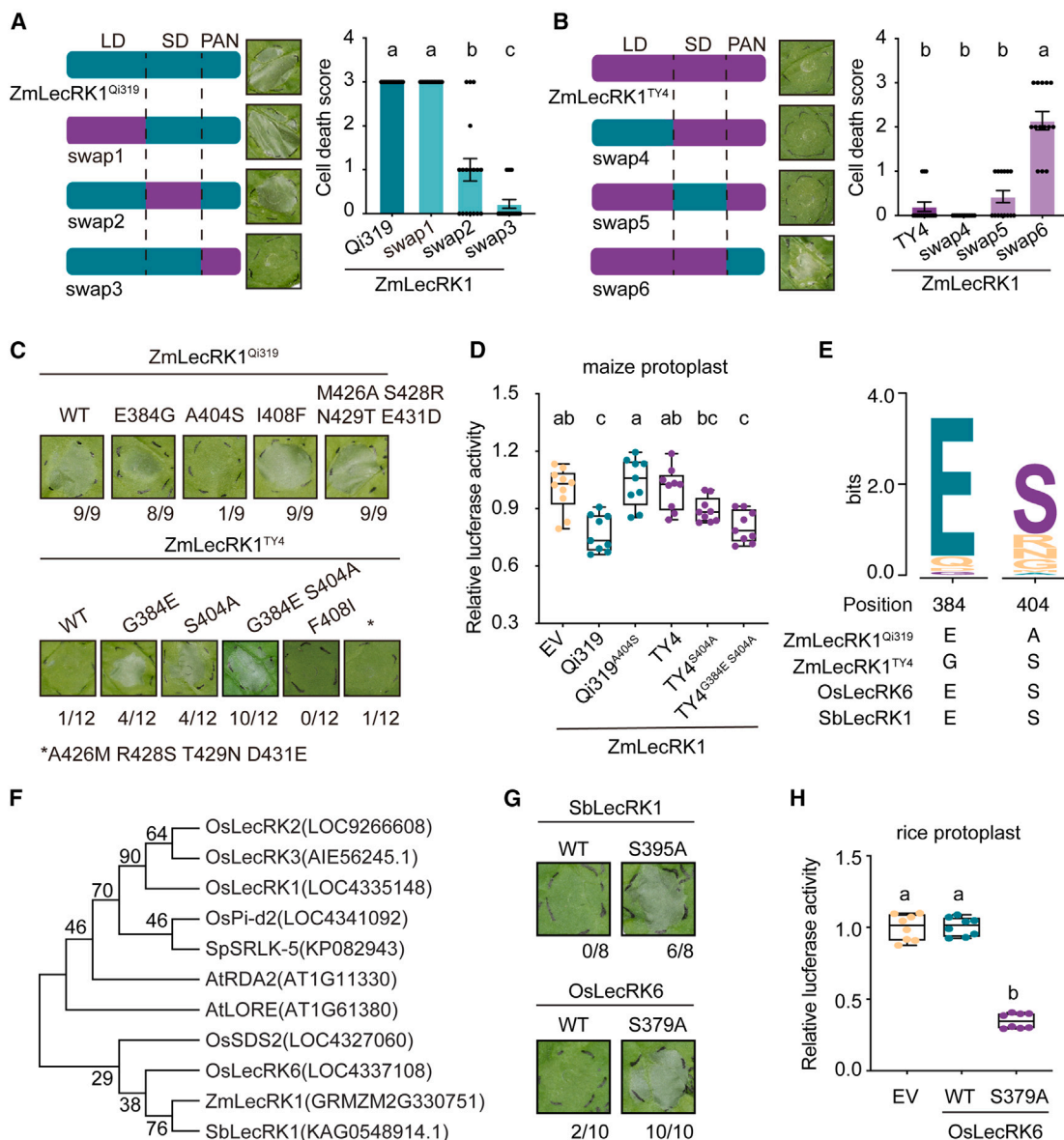


Figure 5. A404 is one of the critical residues for ZmLecRK1-induced cell death.

(A and B) Representative phenotype of *N. benthamiana* leaves expressing mutants and wild-type ZmLecRK1^{QI319} and ZmLecRK1^{TY4}.

(C and D) Cell-death assay of transiently expressing ZmLecRK1^{QI319}, ZmLecRK1^{TY4}, and the corresponding mutants in *N. benthamiana* (C) and maize protoplasts (D).

(E) Frequency of the two key residues E384 and A404 of ZmLecRK1 in the genomes of grass species.

(F) Phylogenetic analysis revealed that ZmLecRK1s are closely related to SbLecRK1 and OsLecRK6.

(G) Substitution of S by A enhances the cell death triggered by SbLecRK1 and OsLecRK6 in *N. benthamiana*.

(H) Substitution of S by A enhances the cell death triggered by OsLecRK6 in rice protoplasts. Numbers on the bottom indicate leaves showing obvious HR over all infiltrated leaves (C and G). Letters indicate significantly different groups, as determined by one-way ANOVA followed by Tukey's test at $\alpha = 0.05$ (A, B, D, and H).

Figure 6C). Furthermore, ZmBAK1 was unable to enhance the self-association of ZmLecRK1^{QI319} with the A404S mutation (Figure 6C). Finally, the BN-PAGE assay showed that the A404S mutation in ZmLecRK1^{QI319} attenuates its ability to form high-order complexes in maize protoplasts (Figure 6D). As expected, overexpressing the ZmLecRK1^{QI319} with the A404S mutation does not cause autoimmunity in *Arabidopsis* (Supplemental Figure 6D). These results together indicate that the A404 residue

is required for the interaction between ZmLecRK1 and ZmBAK1 and the activation of ZmLecRK1.

ZmLecRK1 modulates the pathways related to cell wall organization or biogenesis

To further elucidate the molecular mechanism underlying ZmLecRK1-mediated resistance, we performed an RNA

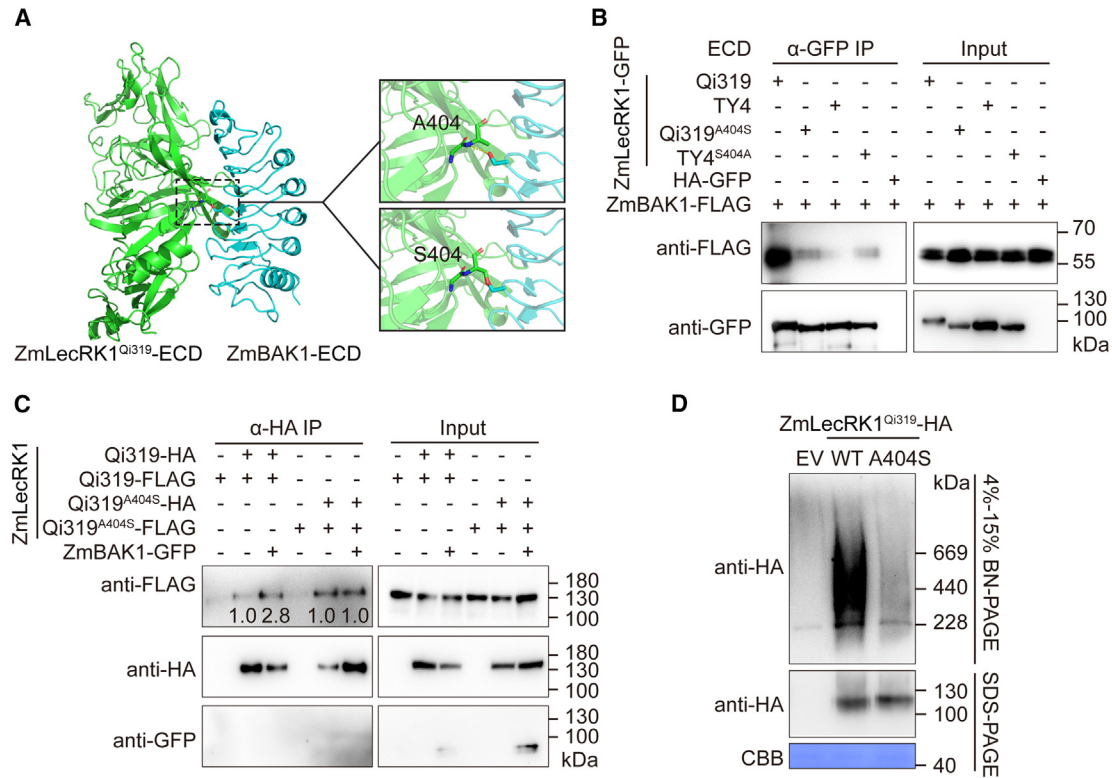


Figure 6. A404S mutation impairs the ZmLecRK1^{Qi319}-ZmBAK1 interaction.

(A) AlphaFold2-Multimer predicted ZmLecRK1^{Qi319}-ECD-ZmBAK1-ECD complex in ColabFold server (parameters: “MMseqs2” and “AlphaFold2-Multimer-v2” pattern). Green and blue indicate the ZmLecRK1^{Qi319} and ZmBAK1, respectively. The stick model represents the potential interface between ZmLecRK1^{Qi319} and ZmBAK1.

(B) Co-IP assay to show that mutation in ZmLecRK1 impairs the ZmLecRK1-ECD-ZmBAK1-ECD interaction.

(C) Effect of ZmBAK1 on the self-interaction strength of ZmLecRK1^{Qi319} and ZmLecRK1^{Qi319} with A404S mutation, as shown by Co-IP in *N. benthamiana*. Numbers on gel blots indicate relative arbitrary densitometry units of corresponding bands after normalization to the sample without ZmBAK1-GFP in grouped samples.

(D) ZmLecRK1^{Qi319} form complexes in an A404-dependent manner, as shown by BN-PAGE and SDS-PAGE.

sequencing (RNA-seq) analysis using field-grown KN5585 and *zmllecrk1-c2* plants infected with one of the fungal pathogen *R. solani* at 72 h post inoculation. In mock-treated maize plants, 298 genes were upregulated and 194 downregulated in *zmllecrk1-c2* compared with KN5585 (Figure 7A and Supplemental Figure 7A; Supplemental Table 5). In plants infected with *R. solani* at 72 h post inoculation, 207 genes were upregulated and 270 downregulated in *zmllecrk1-c2* compared with KN5585 (Figure 7A and 7B; Supplemental Table 6). Gene Ontology (GO) term enrichment analysis revealed that, in the *R. solani*-infected plants, 170 downregulated differentially expressed genes (DEGs) were enriched in a pathway related to stimuli in *zmllecrk1-c2* (Figure 7C). For those upregulated DEGs, they show similar tendency in *zmllecrk1* mutant lines treated with or without pathogen (Figure 7C and Supplemental Figure 7B). This suggests that ZmLecRK1 positively impacts defense-related genes after *R. solani* infection. In addition, GO analysis identified significant enrichment of many DEGs in functional categories associated with cell-wall organization or biogenesis-associated functional categories, including pathways related to xyloglucan metabolism, cellulose metabolism, pectin metabolism, and lignin metabolism (Figure 7C and 7D and Supplemental Figure 7C). These results suggest that

ZmLecRK1 likely plays a role in modulating cell wall organization or biogenesis in response to pathogen infection.

DISCUSSION

Several multi-pathogen resistance genes have been identified in maize. For example, *ZmCCoAOMT2* encodes a caffeoyl-CoA O-methyltransferase that enhances resistance against southern leaf blight (SLB), gray leaf spot (GLS), and NLB through the phenylpropanoid pathway and lignin accumulation (Yang et al., 2017b). *ZmMM1* codes for a transcription repressor, which causes a lesion mimic phenotype and confers resistance to NLB, GLS, and southern corn rust (Wang et al., 2021). *ZmNANMT* is a susceptibility gene to SLB, NLB, and Fusarium stalk rot (Li et al., 2023). Here, we demonstrated that G-type LecRK ZmLecRK1 imparts resistance against Pythium stalk rot, SLB, and banded leaf and sheath blight (BLSB), three major maize diseases (Figure 1 and 3). This resistance is likely mediated through the early-stage stimulation of ROS accumulation and the regulation of gene expression associated with cell-wall organization or biogenesis during later stages of infection (Figure 1 and 7). The allele-specific interactions of ZmLecRK1 with ZmBAK1 revealed that residue A404 of ZmLecRK1 is

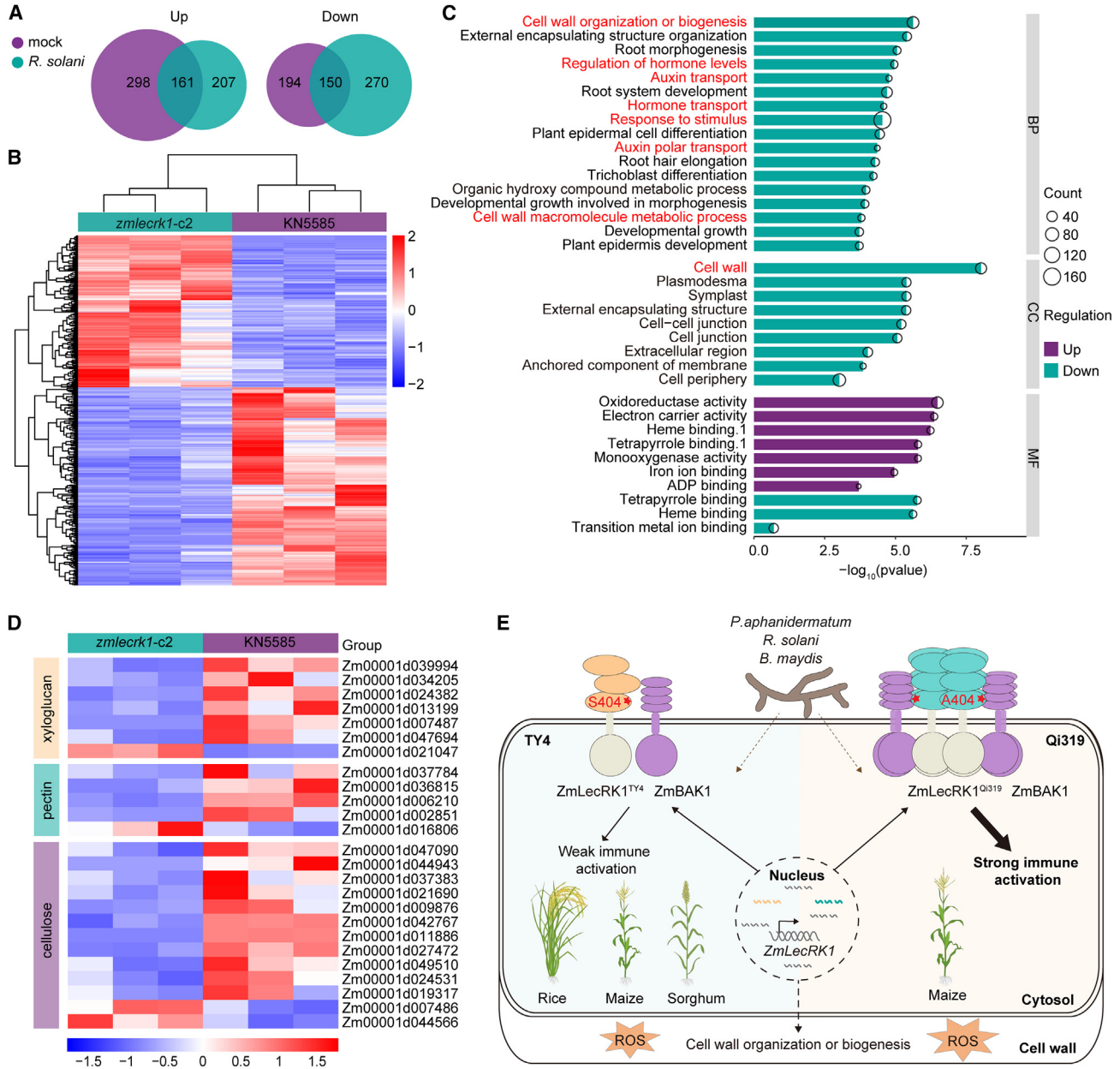


Figure 7. ZmLecRK1 is involved in regulating ROS production and cell-wall organization or biogenesis.

(A) Number of differentially expressed genes (DEGs) identified in KN5585 and *zmlecrk1-c2* infected with mock or *R. solani* at 72 h post inoculation, respectively.

(B) Hierarchical clustering of DEGs in KN5585 and *zmlecrk1-c2* infected with *R. solani* at 72 h post inoculation.

(C) Enrichment analysis of Gene Ontology (GO) pathway terms for the DEGs in KN5585 and *zmlecrk1-c2* infected with *R. solani* at 72 h post inoculation. BP, biological process; CC, cellular component; MF, molecular function.

(D) The heatmap of DEGs in each line that are associated with pathways related to xyloglucan metabolism, pectin metabolism, and cellulose metabolism.

(E) A proposed working model. Upon pathogen invasion, expression of *ZmLecRK1* is induced in both Qi319 and TY4 maize inbred lines and then *ZmLecRK1* positively modulates the accumulation of ROS and cell-wall organization or biogenesis to enhance resistance against multiple diseases. However, compared to *ZmLecRK1*^{TY4}, *ZmLecRK1*^{Qi319} recruits more co-receptors *ZmBAK1* to form immune complexes for stronger immune activation. The A404 is a key residue that distinguishes the *ZmLecRK1* variants. The strong *ZmLecRK1* variant with A404 is a derived mutation specific to maize, with most grass genomes encoding apparently weakly active *ZmLecRK1* homologs with S404.

required for robust downstream immune activation. *ZmLecRK1* homologs are relatively conserved as functionally weak variants with S404 in grass species, with the S404A mutation in *ZmLecRK1* and *ZmLecRK1*-like proteins increasing their ability to induce cell death in maize and rice (Figure 5). We proposed

that the highly active *ZmLecRK1* variant with A404, a derived allele only found in maize, enables it to recruit more co-receptors than the weak *ZmLecRK1* variant with S404, thereby enhancing the formation of immune complexes (Figure 6 and 7E).

For G-type LecRKs, it has not yet been well established how co-receptors contribute to receptor activation and downstream signaling, although several G-type LecRKs are associated with co-receptors BAK1 or SOBIR1 (Pi et al., 2022; Bao et al., 2023). In *Arabidopsis*, receptor homodimerization is essential for LORE-mediated immune signaling, but the responsible domain has yet to be identified (Eschrig et al., 2024). Our study found that the co-receptor ZmBAK1 is genetically required for ZmLecRK1-induced cell death and that the PAN domain-mediated ZmLecRK1-ZmBAK1 interaction is crucial for the complex formation (Figure 3 and 6). The PAN domain, with a core of four to six cysteine residues, is present in over 28 000 proteins across 959 genera (Pal et al., 2022; De et al., 2023). Among these, G-type LecRK is the only plant protein family that contains the PAN domain (Pal et al., 2022; De et al., 2023). The PAN domain of the plasminogen/hepatocyte growth factor family (HGF) acts as a binding site for its receptor, c-MET, which regulates the downstream signaling cascade, including ERK phosphorylation (Pal et al., 2022). Additionally, the PAN domain has been suggested as a key domain for mediating protein-protein or carbohydrate-protein interactions and facilitating receptor dimerization (Herwald et al., 1996; Ho et al., 1998; Zhou et al., 1998; Baglia et al., 2000; Naithani et al., 2007). Our study revealed that the PAN domain is essential for the protein-protein interaction between ZmLecRK1 and its co-receptor ZmBAK1 (Figure 3 and 4), which will advance our understanding of the widely present protein family with the PAN domain in both plants and animals. Additionally, identifying the putative ligands of ZmLecRK1 from plants would further help to understand how the PAN domain mediates ZmLecRK1 activation during plant and microbe interactions.

Several LecRKs have been identified as disease-resistant genes in crops, but not in maize. For example, *Pi-d2*, *SDS2*, and *OsLecRK1-3* mediated disease and pest resistance in rice (Chen et al., 2006; Liu et al., 2015; Fan et al., 2018; Dai et al., 2023), *SpSRLK-5* mediates *Fusarium* wilt disease in tomato (Catanzariti et al., 2015), and *Rph22* and *HvLecRK-V* mediated leaf rust fungi in barley and powdery mildew in wheat (Wang et al., 2018, 2019). Among them, *OsLecRK1* is suggested to be involved in perception of Poaceae-specific DAMP, mixed-linked β -1,3/1,4-glucans (Dai et al., 2023). However, few studies examined natural variations in LecRKs and their effects on phenotypes. Taking advantage of the ZmLecRK1-induced cell death phenotype, we demonstrated that the key residue A404 is crucial for ZmLecRK1 function. The weak variant with S404 is clearly the ancestral variant in other grasses. Although the A404 residue enhances disease resistance, its fitness cost in the field, especially in rice and other grasses, remains unknown. Previous studies showed that the fitness cost of some hyperactive resistance alleles might be genetic background dependent (Yang and Hua, 2004; Chintamanani et al., 2010; Olukolu et al., 2013, 2014; Zhu et al., 2018; Chen et al., 2023b). Therefore, there is also the possibility that compensatory epistatic changes at other loci, which are present in maize but not other grasses, may be required to mitigate any negative effects of the A404 substitution. In the future, precisely editing the S404 residue of ZmLecRK1 and its homologs in different grass species will help to understand the fitness of both alleles in the field. In addition, further investigations are required to determine whether other

mutations at position 404 in other species could confer resistance (Supplemental Figure 5E).

In summary, we identified *ZmLecRK1* as a multi-pathogen resistance gene in maize. ZmLecRK1 interacts with the co-receptor ZmBAK1 to form an immune complex for defense. The natural variation within ZmLecRK1, specifically the S404A substitution, significantly enhances disease resistance through stronger interactions with its co-receptor ZmBAK1, highlighting the biotechnological potential of precisely modulating the activity of ZmLecRK1 and its homologs in maize and rice for resistance to multiple pathogens through targeted base editing.

METHODS

Plant materials and growth conditions

Maize inbred lines were obtained from the National Maize Improvement Centre of China, China Agricultural University (Beijing, China), and gene-editing maize materials were generated by Wimibio (Jiangsu, China). All seeds were germinated at 25°C in the dark for 3 days in a shallow dish covered by water-soaked blotting paper. Seeds with consistent germination were selected for subsequent experiments.

A. thaliana transgenic lines were derived from Col-0. Plants were surface sterilized with 75% ethanol and 0.1% Tween 20 for 10 min, washed thoroughly in absolute ethanol for 3 min, then dried in an ultra-clean workbench before being sown in soil or germinated on 1/2 Murashige and Skoog solid medium (pH 5.7) and grown under long-day (16 h day/8 h night) regimes at 23°C with relative humidity at 65%. Four-week-old plants were used for most experiments in this study.

N. benthamiana plants were grown in a greenhouse at 25°C with long-day (16 h day/8 h night) conditions for 4–5 weeks.

Constructs and transgenic lines

ZmLecRK1 (GRMZM2G330751) fragment was amplified from Qi319 and TY4 DNA with PCR primers designed based on the ZmLecRK1-B73 sequence. *ZmBAK1* (GRMZM2G145720) fragment was amplified from B73 cDNA. *OsLecRK6* (GenBank: LOC4337108) fragment was amplified from Nipponbare cDNA. *SbLecRK1* (GenBank: KAG0548914.1) fragment was amplified from sweet sorghum E048 genomic DNA with PCR primers designed based on the KAG0548914.1 sequence. For transient expression in maize protoplasts, the ZmLecRK1 coding sequences were cloned into a modified pUC19 vector. For transient expression in *N. benthamiana*, pCBCS vectors with the cauliflower mosaic virus (CaMV) 35S promoter were used. The expression constructs were introduced into *Agrobacterium tumefaciens* GV3101 by electroporation. Stable transgenic *Arabidopsis* plants were generated through the floral dipping method. T1 transformants were screened based on basta selection. All gene-editing maize materials were generated by *Agrobacterium*-mediated transformation using calli from the maize inbred line KN5585 as the recipients (Wimi Biotechnology). Homozygote editing lines were confirmed by Sanger sequencing. Primers used in this section are listed in Supplemental Table 7.

Molecular Plant

Natural variations of maize ZmLecRK1 in disease resistance

Pathogen inoculation in greenhouse

Pythium aphanidermatum was grown on V8 plates at 25 °C in the dark for 2 days. *P. aphanidermatum* inoculation assays on detached leaves were performed as previously described (Liu et al., 2024). *R. solani* strain was grown on potato-dextrose-agar medium at 25 °C for 2 days. Infection assays on maize with *R. solani* were performed by inoculating fresh mycelial plugs ($\Phi = 6$ mm) on the fourth leaf. Inoculated leaves were kept in a climate chamber at 25 °C for 1–2 days. Percentage of necrotic leaf area was measured at 36 h post infection. *B. maydis* was grown on potato-dextrose-agar medium at 25 °C for 21 days. Spores were collected by sterilized water with 0.1% Tween 20 and $2.5\text{--}3.0 \times 10^5$ spores/ml. Approximately 5 ml of spore culture was sprayed on each pot to ensure the spores were sprayed evenly onto the fourth leaf. After inoculation, the inoculated plants were kept at 95% humidity for 1 day then moved to the growth room for 6 days of disease development.

Pathogen inoculation in the field

P. aphanidermatum was cultured as described above. The mycelia were washed with sterile water and submerged with sterile water in Petri dish in the dark for 24 h to induce sporocarps. Five milliliters of Petri's salt solution (1.1 mM KH_2PO_4 , 0.6 mM $\text{MgSO}_4 \cdot 7\text{H}_2\text{O}$, 0.8 mM KCl, 2.4 mM $\text{Ca}(\text{NO}_3)_2$) were added to the Petri dish. After 4 h, the solution was replaced with another 5 ml of PS solution. Zoospores were harvested 6–8 h later. At the tasseling stage, the third internode from the base of the plants was drilled and inoculated by a 20- μl suspension ($2 \times 10^5/\text{ml}$) of zoospores. Lesion length was measured after 3 weeks post inoculation. For BLSB, 12 plugs ($\Phi = 6$ mm) were taken from the edge of the culture and placed in a conical flask containing 200 ml of potato-dextrose liquid medium at 25 °C with shaking at 180 rpm for 3 days. Subsequently, the hyphae were mechanically crushed and used as an inoculum. A 2-cm-wide filter paper strip was thoroughly soaked in the inoculum and gently wound around the fourth plant sheaths at the V9–V10 stage. The strip was secured with grafting tape to maintain moisture. Lesion length and severity were measured at 14 days post inoculation in the field. For SLB inoculation in the field, the method described by Sermons and Balint-Kurti (Sermons and Balint-Kurti, 2018) was followed. In the Fusarium stalk rot infection assay, maize stalks were drilled at the third, fourth, or fifth internode using a sterile micropipette tip, followed by injection of a 20- μl spore suspension ($1 \times 10^6/\text{ml}$) of *F. graminearum*. Lesion length was measured 2 weeks post inoculation.

ROS burst detection

Leaf discs were excised from KN5585 and *zmlcck1* plants at the two-third leaf stage using a 4-mm-diameter punch and incubated in 200 μl of water in a 96-well white plate overnight. At least eight plants per line were sampled. Next, water was replaced by 100 μl of $2 \times \text{L-012}$ (Wako, Chuo-ku, Japan; 15 mg of L-012 in 1 ml of 200 mM KOH is $100 \times \text{L-012}$). Then 100 μl of buffer containing $2 \times$ horseradish peroxidase (HRP) buffer (Solarbio Life Science, Beijing, China; 25 mg of HRP in 2.5 ml is $100 \times \text{HRP}$) was added into the reactions. One was used for the PAMP treatment group with 2.5 μM flg22 or 25 mg/ml chitin; the other was used for mock control without PAMPs. The luminescence was recorded

every 46 s for 1 h using a microplate reader (BioTek Synergy H1, Agilent, CA, USA).

Cell-death assays in *N. benthamiana* leaves and protoplasts

For the cell-death assays, *A. tumefaciens* GV3101 harboring *35S::ZmLecRK1^{Qi319}-FLAG-TurboID*, *35S::ZmLecRK1^{TY4}-FLAG-TurboID*, or *35S::FLAG-TurboID* was infiltrated into *N. benthamiana* leaves. Leaves were scored between 48 and 72 h post infiltration for a visible cell-death phenotype.

Luciferase activity in maize protoplasts was used to indicate host cell death triggered by ZmLecRK1^{Qi319}, ZmLecRK1^{TY4}, or its mutants. The activity was measured by using the luciferase assay system, which was performed 16 h after transfection with the plasmid combinations containing ZmLecRK1^{Qi319} and ZmLecRK1^{TY4} or its mutants. Maize protoplasts were prepared from ZhengDan958, KN5585, or *zmbak1* leaves as described previously (Liu et al., 2024), rice protoplasts were prepared from Nipponbare leaf sheaths, and the plasmid combinations mixed with the empty and LUC plasmids were co-transfected into maize or rice protoplasts via the poly(ethylene glycol) method. After transient expression, all the protoplasts were collected, the supernatants were discarded by pipette, and 100 μl of luciferase cell culture lysis buffer (25mM Tris-phosphate [pH 7.8], 2 mM 1,2-diamino cyclohexane-N,N,N',N'-tetraacetic acid, 10% glycerol, 1% Triton X-100, 2 mM DTT) was used to lyse the protoplasts on ice. Twenty microliters of lysate, 20 μl ATP buffer (125 mM Tris-HCl [pH 7.5], 25 mM MgCl_2 , 4 mM ATP), and 40 μl 2 mM luciferin were mixed, and the chemiluminescence was recorded using a microplate reader. The strength of the chemiluminescence reflected the amount of luciferase, which was influenced by the number of live protoplasts. The lower the chemiluminescence signal, the fewer the live protoplasts, and the value in the control group was used to reflect the transformation efficiency.

qPCR

RNA was extracted from plant tissue using an RNA isolation method (R401, Vazyme Biotech, Nanjing, China). cDNA was synthesized from 0.5 mg of high-quality total RNA ($\text{A260}/\text{A230} > 2.0$ and $\text{A260}/\text{A280} > 1.8$), using HiScript III First Strand cDNA Synthesis (R312, Vazyme Biotech, Nanjing, China). SYBR master mix (Q711, Vazyme Biotech, Nanjing, China) was used for real-time qPCR in a Thermo Fisher system (ABI QuantStudio 6 Flex) according to the manufacturer's instructions. The comparative $2^{-\Delta\Delta\text{Ct}}$ method was used to calculate the relative expression of genes of interest, using *AtACT2*, *Zm18S*, or *ZmActin* gene as an internal control. The primers used for qPCR are listed in Supplemental Table 7.

In vitro phosphorylation assay

ZmLecRK-KD and ZmLecRK1-KD^{K548R} were cloned into the pET-1a 6 \times His MBP FLAG expression vector to produce MBP-tagged recombinant proteins (MBP-ZmLecRK-KD and MBP-ZmLecRK1-KD^{K548R}) in *Escherichia coli* BL21. Protein purification was performed using the method described by Chen et al. (2023b). For *in vitro* phosphorylation assay, the recombinant proteins were incubated in kinase buffer (20 mM Tris-HCl pH7.5, 10 mM MgCl_2 , 1 mM DTT) in the presence of 1 mM ATP

for 30 min at 30°C. The reactions were stopped by adding 5× SDS loading buffer (250 mM Tris-HCl pH 6.8, 10% SDS, 0.5% bromophenol blue, 50% glycerol, 5% β-mercaptoethanol). Proteins were separated by SDS-PAGE, followed by staining with CBB. The level of the phosphorylation status of fusion proteins was detected by Phos-tag Biotin (BTL-104, NARD, Japan) and streptavidin-HRP (550946, BD, USA).

Immunoprecipitation-MS

The immune complexes were analyzed by MS at the China Agricultural University Mass Spectrum Laboratory. Briefly, 3 mg of ZmLecRK1^{Qi319}-FLAG plasmids were transformed into 50 ml of maize protoplasts, which were prepared from KN5585 and incubated for 18 h. The FLAG-tagged fusion protein complex was extracted by 50 μl of FLAG beads and subjected to digestion with trypsin. After tryptic digestion, peptides were extracted and redissolved in 25 μl (0.1%) of trifluoroacetic acid. In total, 6 μl of extracted peptides were analyzed using an LTQ Orbitrap Velos mass spectrometer (Thermo Fisher Scientific). The Mascot search engine Mascot Server 2.3 (Matrix Science) was used for protein identification by searching against the UniProt protein database (<https://www.uniprot.org/>). The false discovery rate (FDR) was also set to 0.01 for protein identifications. The significance threshold was set at $p < 0.05$, and a minimum number of significant unique sequences was set to 1.

Phylogenetic analysis

The amino acid sequences of ZmBAK1 homologs were downloaded from the National Center for Biotechnology Information (NCBI) database (<https://www.ncbi.nlm.nih.gov/>). Sequences were aligned with Jalview (Waterhouse et al., 2009), and the phylogenetic tree was developed using MEGA 11 (Tamura et al., 2021). The evolutionary history was inferred using the neighbor-joining method. The optimal tree is shown. The percentages of replicate trees in which the associated taxa clustered together in the bootstrap test (1000 replicates) are shown next to the branches. The evolutionary distances were computed using the p-distance method and are in the units of the number of amino acid differences per site. This analysis involved 13 amino acid sequences. All ambiguous positions were removed for each sequence pair (pairwise deletion option). There were a total of 643 positions in the final dataset.

Protein homology search and alignment

The amino acid sequences of ZmLecRK1 homologs in Gramineae were downloaded from the NCBI (<https://www.ncbi.nlm.nih.gov/>). The G-type LecRK in maize amino acid sequences were retrieved from the MaizeGDB database (<https://www.maizegdb.org/>). The protein sequences of 251 OsLecRK6 homologs were retrieved from a rice pangenomic database (Shang et al., 2022). Multiple-sequence alignments of proteins were performed in Jalview using GLprobs (<https://www.jalview.org/>). Sequence LOGOs of ZmLecRK1^{Qi319}, ZmLecRK1^{TY4}, SbLecRK1, and OsLecRK6 in Gramineae were created by WebLOGO webserver with PAN domain (Crooks et al., 2004).

VIGS in *N. benthamiana*

VIGS was performed based on TRV (Liu et al., 2002). *A. tumefaciens* cultures containing the constructed TRV2 vector

were mixed with *A. tumefaciens* cultures containing the constructed TRV1 vector in a 1:1 ratio in the infiltration solution (10 mM MgCl₂, 10 mM MES pH 5.7) to a final optical density 600 of 0.25. TRV2:GFP and TRV2:PDS were used as controls. The efficiency of gene silencing was determined by qPCR. The experiments were repeated three times. Primers used in this study are listed in Supplemental Table 7.

BN-PAGE

BN-PAGE was performed as previously described (Wang et al., 2023a). Three 14-day-old *Arabidopsis* seedlings and maize protoplasts overexpressing ZmLecRK1 were collected and homogenized in 1× NativePAGE Sample Buffer (BN20032, Invitrogen, CA, USA) supplemented with 1% n-dodecyl β-D-maltoside and protease inhibitor cocktail (4693116001, Roche, USA). Homogenization was achieved by gently mixing on ice for 20 min, followed by 20 000 g centrifugation for 15 min at 4°C. The resulting supernatant was mixed with 0.25% G-250 Sample Additive and loaded on a NativePAGE 4%–15% Bis-Tris gel (BN1001BOX, Invitrogen, CA, USA) for electrophoresis.

SLC assay

In the split-Luc assays, ZmBAK1-nLuc was transiently co-expressed with ZmLecRK1^{Qi319}-cLuc, ZmLecRK1^{TY4}-cLuc, and empty vector control (EV) in 4-week-old *N. benthamiana* leaves. At 2 days post infiltration with *Agrobacterium* strains harboring the relevant constructs, leaves were infiltrated with 1 mM luciferin containing 0.02% Silwet L-77 and kept in the dark for 10 min before charge-coupled device imaging. To quantify the luciferase signal, leaf discs were collected from the inoculated leaves using a 6-mm punch and placed into a 96-well plate with 25 μl of H₂O. Twenty-five microliters of 2 mM luciferin were added to the leaf discs in the 96-well plate before recording luminescence. To determine pathogen and PAMP-induced protein-protein interaction, 25 μl of *P. aphanidermatum* solution or 200 μg/ml chitin with 2 mM luciferin was added before recording.

Co-IP

N. benthamiana leaves were used for *A. tumefaciens*-mediated transient protein expression. Typically, the samples were harvested at 48 h post infiltration. Ground tissues were homogenized in ice-cold extraction buffer (10% glycerol, 25 mM Tris-HCl pH 7.5, 1 mM EDTA, 150 mM NaCl, 2% PVP, 0.5% Triton-X100) supplemented with 1 mM DTT, anti-protease tablet (04693132001, Roche, USA). The resulting lysate was homogenized by mixing for 20 min on ice and centrifuged at 13 000 rpm for 15 min at 4°C, with this step being repeated twice. The supernatant was incubated with 5 μl of antibodies-coupled beads (Anti-FLAG M2, M8823, Sigma-Aldrich, USA; Anti-HA, KTSM1335, KangTi Life Technology, Shenzhen, China; Anti-GFP, KTSM1334, KangTi Life Technology, Shenzhen, China) for 3 h at 4°C under gentle agitation. After incubation, beads were washed six times with washing buffer (25 mM Tris-HCl pH 7.5, 1 mM EDTA, 150 mM NaCl, 0.5% Triton-X 100, 1 mM DTT) at 4°C. SDS loading buffer (8 M urea, 2% SDS, 20% glycerol, 100 mM Tris-HCl pH 6.8, 0.004% bromophenol blue) with 100 mM DTT was added to the beads before boiling at 95°C for 5 min to release bound proteins. Released proteins were analyzed by immunoblots with anti-FLAG M2-HRP (A8592,

Molecular Plant

Merck, USA), anti-HA-HRP (12013819001, Roche, USA), or anti-GFP (AE012, ABclonal, Wuhan, China) antibodies.

RNA-seq analysis

We used plant sheath samples at the V9–V10 stage of the *zmlcck1-c2* and KN5585 for RNA-seq in this transcriptomic study. The plant sheaths of the *zmlcck1-c2* and KN5585 were inoculated with *R. solani* inoculum or mock solution as described in the field experiments. The samples were sent to Tsingke Biotechnology (Beijing, China) for RNA-seq by using the DNBSEQ platform. The DEG analysis was performed using DESeq2, and a threshold of $|\log_2(\text{FC})| > 1$, $p_{\text{adj}} < 0.05$ was used to screen DEGs. GO analysis was performed using AgriGov2 (<http://systemsbiology.cau.edu.cn/agriGOv2/index.php>) (Tian et al., 2017), and biological pathways with an FDR < 0.001 were confirmed to be enriched.

DATA AND CODE AVAILABILITY

All data and materials needed to repeat the work are available. RNA-seq raw data have been deposited at the NCBI under BioProject accession PRJNA1161467.

FUNDING

This work was supported by Biological Breeding-National Science and Technology Major Project (no. 2023ZD04070, W.Z.), the National Key Research and Development Program, Ministry of Science and Technology of China (no. 2022YFD1201802, W.Z.), the National Natural Science Foundation of China (no. 32472499, W.Z.), and the Pinduoduo-China Agricultural University Research Fund (no. PC2023A01005, Y.-L.P.).

ACKNOWLEDGMENTS

We thank Detlef Weigel, Bo Li, Guozhi Bi, Xiagnxiu Liang, Guangyuan Xu, Ning Xu, Xin Zhang, and three anonymous reviewers for their valuable comments and advice on this manuscript. We thank Daolong Dou for *P. aphandermatum* and the VIGS toolkit for *N. benthamiana*, Xujun Chen for *R. solani*, Wende Liu for *B. maydis*, Canxing Duan for *F. graminearum*, Guanfeng Wang for Rp1-D21 plasmid, Feifei Yu for sorghum genomic DNA. No conflict of interest is declared.

AUTHOR CONTRIBUTIONS

Conceptualization, Z.L., J.C., and W.Z.; methodology, L.W., S.W., Y.-L.P., M.X., and X.Y.; formal analysis, Z.L., J.C., and W.Z.; investigation, Z.L., J.C., C.L., S.H., W.C., H.L., and W.Z.; writing – original draft, Z.L.; writing – review & editing, J.C. and W.Z.; supervision, W.Z.; project administration, W.Z.; funding acquisition, W.Z.

SUPPLEMENTAL INFORMATION

Supplemental information is available at *Molecular Plant Online*.

Received: June 12, 2024

Revised: August 28, 2024

Accepted: September 18, 2024

Published: September 19, 2024

REFERENCES

- Baglia, F.A., Badellino, K.O., Ho, D.H., Dasari, V.R., and Walsh, P.N. (2000). A binding site for the kringle II domain of prothrombin in the apple 1 domain of factor XI. *J. Biol. Chem.* **275**:31954–31962.
- Balint-Kurti, P.J., and Johal, G.S. (2009). Maize disease resistance. In *Handbook of Maize: Its Biology*, J.L. Bennetzen and S.C. Hake, eds. (Springer), pp. 229–250.
- Bao, Y., Li, Y., Chang, Q., Chen, R., Wang, W., Zhang, Q., Chen, S., Xu, G., Wang, X., Cui, F., et al. (2023). A pair of G-type lectin receptor-like

Natural variations of maize ZmLecRK1 in disease resistance

kinases modulates nlp20-mediated immune responses by coupling to the RLP23 receptor complex. *J. Integr. Plant Biol.* **65**:1312–1327.

Boller, T., and Felix, G. (2009). A renaissance of elicitors: perception of microbe-associated molecular patterns and danger signals by pattern-recognition receptors. *Annu. Rev. Plant Biol.* **60**:379–406.

Cao, H., Yang, Z., Song, S., Xue, M., Liang, G., and Li, N. (2022). Transcriptome analysis reveals genes potentially related to maize resistance to *Rhizoctonia solani*. *Plant Physiol. Biochem.* **193**:78–89.

Catanzariti, A.-M., Lim, G.T.T., and Jones, D.A. (2015). The tomato I-3 gene: a novel gene for resistance to *Fusarium* wilt disease. *New Phytol.* **207**:106–118.

Chen, X., Shang, J., Chen, D., Lei, C., Zou, Y., Zhai, W., Liu, G., Xu, J., Ling, Z., Cao, G., et al. (2006). A B-lectin receptor kinase gene conferring rice blast resistance. *Plant J.* **46**:794–804.

Chen, L.-J., Wuriyangan, H., Zhang, Y.-Q., Duan, K.-X., Chen, H.-W., Li, Q.-T., Lu, X., He, S.-J., Ma, B., Zhang, W.-K., et al. (2013). An S-domain receptor-like kinase, OsSIK2, confers abiotic stress tolerance and delays dark-induced leaf senescence in rice. *Plant Physiol.* **163**:1752–1765.

Chen, C., Zhao, Y., Tabor, G., Nian, H., Phillips, J., Wolters, P., Yang, Q., and Balint-Kurti, P. (2023a). A leucine-rich repeat receptor kinase gene confers quantitative susceptibility to maize southern leaf blight. *New Phytol.* **238**:1182–1197.

Chen, J., Li, L., Kim, J.H., Neuhäuser, B., Wang, M., Thelen, M., Hilleary, R., Chi, Y., Wei, L., Venkataramani, K., et al. (2023b). Small proteins modulate ion-channel-like ACD6 to regulate immunity in *Arabidopsis thaliana*. *Mol. Cell* **83**:4386–4397.e9.

Cheng, X., Wu, Y., Guo, J., Du, B., Chen, R., Zhu, L., and He, G. (2013). A rice lectin receptor-like kinase that is involved in innate immune responses also contributes to seed germination. *Plant J.* **76**:687–698.

Chinchilla, D., Bauer, Z., Regenass, M., Boller, T., and Felix, G. (2006). The Arabidopsis receptor kinase FLS2 binds flg22 and determines the specificity of flagellin perception. *Plant Cell* **18**:465–476.

Chinchilla, D., Zipfel, C., Robatzek, S., Kemmerling, B., Nürnberger, T., Jones, J.D.G., Felix, G., and Boller, T. (2007). A flagellin-induced complex of the receptor FLS2 and BAK1 initiates plant defence. *Nature* **448**:497–500.

Chintamanani, S., Hulbert, S.H., Johal, G.S., and Balint-Kurti, P.J. (2010). Identification of a maize locus that modulates the hypersensitive defense response, using mutant-assisted gene identification and characterization. *Genetics* **184**:813–825.

Couto, D., and Zipfel, C. (2016). Regulation of pattern recognition receptor signalling in plants. *Nat. Rev. Immunol.* **16**:537–552.

Crooks, G.E., Hon, G., Chandonia, J.-M., and Brenner, S.E. (2004). WebLogo: a sequence logo generator. *Genome Res.* **14**:1188–1190.

Dai, Y.-S., Liu, D., Guo, W., Liu, Z.-X., Zhang, X., Shi, L.-L., Zhou, D.-M., Wang, L.-N., Kang, K., Wang, F.-Z., et al. (2023). Poaceae-specific β -1,3;1,4-d-glucans link jasmonate signalling to OsLecRK1-mediated defence response during rice-brown planthopper interactions. *Plant Biotechnol. J.* **21**:1286–1300.

De, K., Pal, D., Shanks, C.M., Yates, T.B., Feng, K., Jawdy, S.S., Hassan, M.M., Prabhakar, P.K., Yang, J.-Y., Chapla, D., et al. (2023). The Plasminogen-Apple-Nematode (PAN) domain suppresses JA/ET defense pathways in plants. *bioRxiv*, published June 18, 2023. <https://doi.org/10.1101/2023.06.15.545202>.

DeFalco, T.A., and Zipfel, C. (2021). Molecular mechanisms of early plant pattern-triggered immune signaling. *Mol. Cell* **81**:4346.

Domazakis, E., Wouters, D., Visser, R.G.F., Kamoun, S., Joosten, M.H.A.J., and Vleeshouwers, V.G.A.A. (2018). The ELR-SOBIR1 complex functions as a two-component receptor-like kinase to

- mount defense against *Phytophthora infestans*. *Mol. Plant Microbe Interact.* **31**:795–802.
- Eschrig, S., Schäffer, M., Shu, L.-J., Illig, T., Eibel, S., Fernandez, A., and Ranf, S.** (2024). LORE receptor homomerization is required for 3-hydroxydecanoic acid-induced immune signaling and determines the natural variation of immunosensitivity within the *Arabidopsis* genus. *New Phytol.* **242**:2163–2179, Advance Access published March 26, 2024. <https://doi.org/10.1111/nph.19715>.
- Fan, J., Bai, P., Ning, Y., Wang, J., Shi, X., Xiong, Y., Zhang, K., He, F., Zhang, C., Wang, R., et al.** (2018). The monocot-specific receptor-like kinase SDS2 controls cell death and immunity in rice. *Cell Host Microbe* **23**:498–510.e5.
- Gilardoni, P.A., Hettenhausen, C., Baldwin, I.T., and Bonaventure, G.** (2011). *Nicotiana attenuata* LECTIN RECEPTOR KINASE1 suppresses the insect-mediated inhibition of induced defense responses during *Manduca sexta* herbivory. *Plant Cell* **23**:3512–3532.
- Gómez-Gómez, L., and Boller, T.** (2000). FLS2: an LRR receptor-like kinase involved in the perception of the bacterial elicitor flagellin in *Arabidopsis*. *Mol. Cell* **5**:1003–1011.
- Gou, M., Balint-Kurti, P., Xu, M., and Yang, Q.** (2023). Quantitative disease resistance: Multifaceted players in plant defense. *J. Integr. Plant Biol.* **65**:594–610.
- Herwald, H., Renné, T., Meijers, J.C., Chung, D.W., Page, J.D., Colman, R.W., and Müller-Esterl, W.** (1996). Mapping of the discontinuous kininogen binding site of prekallikrein. A distal binding segment is located in the heavy chain domain A4. *J. Biol. Chem.* **271**:13061–13067.
- Ho, D.H., Badellino, K., Baglia, F.A., and Walsh, P.N.** (1998). A binding site for heparin in the apple 3 domain of factor XI. *J. Biol. Chem.* **273**:16382–16390.
- Huang, J., Yang, L., Yang, L., Wu, X., Cui, X., Zhang, L., Hui, J., Zhao, Y., Yang, H., Liu, S., et al.** (2023). Stigma receptors control intraspecies and interspecies barriers in Brassicaceae. *Nature* **614**:303–308.
- Hurni, S., Scheuermann, D., Krattinger, S.G., Kessel, B., Wicker, T., Herren, G., Fitze, M.N., Breen, J., Presterl, T., Ouzunova, M., and Keller, B.** (2015). The maize disease resistance gene *Htn1* against northern corn leaf blight encodes a wall-associated receptor-like kinase. *Proc. Natl. Acad. Sci. USA* **112**:8780–8785.
- Ivanov, R., Fobis-Loisy, I., and Gaude, T.** (2010). When no means no: guide to Brassicaceae self-incompatibility. *Trends Plant Sci.* **15**:387–394.
- Jany, E., Nelles, H., and Goring, D.R.** (2019). The molecular and cellular regulation of Brassicaceae self-incompatibility and self-pollen rejection. *Int. Rev. Cell Mol. Biol.* **343**:1–35.
- Jinjun, Z., Peina, J., Fang, Z., Chongke, Z., Bo, B., Yaping, L., Haifeng, W., Fan, C., and Xianzhi, X.** (2020). OsSRK1, an atypical S-receptor-like kinase positively regulates leaf width and salt tolerance in rice. *Rice Sci.* **27**:133–142.
- Jones, J.D.G., and Dangl, J.L.** (2006). The plant immune system. *Nature* **444**:323–329.
- Kato, H., Nemoto, K., Shimizu, M., Abe, A., Asai, S., Ishihama, N., Matsuoka, S., Daimon, T., Ojika, M., Kawakita, K., et al.** (2022). Recognition of pathogen-derived sphingolipids in *Arabidopsis*. *Science* **376**:857–860.
- Kemmerling, B., Schwedt, A., Rodriguez, P., Mazzotta, S., Frank, M., Qamar, S.A., Mengiste, T., Betsuyaku, S., Parker, J.E., Müssig, C., et al.** (2007). The BRI1-associated kinase 1, BAK1, has a brassinolide-independent role in plant cell-death control. *Curr. Biol.* **17**:1116–1122.
- Kutschera, A., Dawid, C., Gisch, N., Schmid, C., Raasch, L., Gerster, T., Schäffer, M., Smakowska-Luzan, E., Belkhadir, Y., Vlot, A.C., et al.** (2019). Bacterial medium-chain 3-hydroxy fatty acid metabolites trigger immunity in *Arabidopsis* plants. *Science* **364**:178–181.
- Labbé, J., Muchero, W., Czarnecki, O., Wang, J., Wang, X., Bryan, A.C., Zheng, K., Yang, Y., Xie, M., Zhang, J., et al.** (2019). Mediation of plant-mycorrhizal interaction by a lectin receptor-like kinase. *Nat. Plants* **5**:676–680.
- Li, Y.-J., Gu, J.-M., Ma, S., Xu, Y., Liu, M., Zhang, C., Liu, X., and Wang, G.-F.** (2023). Genome editing of the susceptibility gene *ZmNANMT* confers multiple disease resistance without agronomic penalty in maize. *Plant Biotechnol. J.* **21**:1525–1527.
- Liu, Y., Schiff, M., Marathe, R., and Dinesh-Kumar, S.P.** (2002). Tobacco Rar1, EDS1 and NPR1/NIM1 like genes are required for N-mediated resistance to tobacco mosaic virus. *Plant J* **30**:415–429.
- Liu, Y., Wu, H., Chen, H., Liu, Y., He, J., Kang, H., Sun, Z., Pan, G., Wang, Q., Hu, J., et al.** (2015). A gene cluster encoding lectin receptor kinases confers broad-spectrum and durable insect resistance in rice. *Nat. Biotechnol.* **33**:301–305.
- Liu, C., Dong, X., Xu, Y., Dong, Q., Wang, Y., Gai, Y., and Ji, X.** (2021). Transcriptome and DNA methylome reveal insights into *Phytoplasma* infection responses in mulberry (*Morus multicaulis* Perr.). *Front. Plant Sci.* **12**:697702.
- Liu, C., He, S., Chen, J., Wang, M., Li, Z., Wei, L., Chen, Y., Du, M., Liu, D., Li, C., et al.** (2024). A dual-subcellular localized β -glucosidase confers pathogen and insect resistance without a yield penalty in maize. *Plant Biotechnol. J.* **22**:1017–1032.
- Luo, X., Wu, W., Liang, Y., Xu, N., Wang, Z., Zou, H., and Liu, J.** (2020). Tyrosine phosphorylation of the lectin receptor-like kinase LORE regulates plant immunity. *EMBO J.* **39**:e102856.
- Ma, X., Xu, G., He, P., and Shan, L.** (2016). SERKING coreceptors for receptors. *Trends Plant Sci.* **21**:1017–1033.
- Macho, A.P., and Zipfel, C.** (2014). Plant PRRs and the activation of innate immune signaling. *Mol. Cell* **54**:263–272.
- Mirdita, M., Schütze, K., Moriwaki, Y., Heo, L., Ovchinnikov, S., and Steinegger, M.** (2022). ColabFold: making protein folding accessible to all. *Nat. Methods* **19**:679–682.
- Mondal, R., Biswas, S., Srivastava, A., Basu, S., Trivedi, M., Singh, S.K., and Mishra, Y.** (2021). In silico analysis and expression profiling of S-domain receptor-like kinases (SD-RLKs) under different abiotic stresses in *Arabidopsis thaliana*. *BMC Genom.* **22**:817.
- Naithani, S., Chookajorn, T., Ripoll, D.R., and Nasrallah, J.B.** (2007). Structural modules for receptor dimerization in the S-locus receptor kinase extracellular domain. *Proc. Natl. Acad. Sci. USA* **104**:12211–12216.
- Ngou, B.P.M., Wyler, M., Schmid, M.W., Kadota, Y., and Shirasu, K.** (2024). Evolutionary trajectory of pattern recognition receptors in plants. *Nat. Commun.* **15**:308.
- Olukolu, B.A., Negeri, A., Dhawan, R., Venkata, B.P., Sharma, P., Garg, A., Gachomo, E., Marla, S., Chu, K., Hasan, A., et al.** (2013). A connected set of genes associated with programmed cell death implicated in controlling the hypersensitive response in maize. *Genetics* **193**:609–620.
- Olukolu, B.A., Wang, G.-F., Vontimitta, V., Venkata, B.P., Marla, S., Ji, J., Gachomo, E., Chu, K., Negeri, A., Benson, J., et al.** (2014). A genome-wide association study of the maize hypersensitive defense response identifies genes that cluster in related pathways. *PLoS Genet.* **10**:e1004562.
- Pal, D., De, K., Shanks, C.M., Feng, K., Yates, T.B., Morrell-Falvey, J., Davidson, R.B., Parks, J.M., and Muchero, W.** (2022). Core cysteine residues in the Plasminogen-Appl-Nematode (PAN) domain are critical for HGF/c-MET signaling. *Commun. Biol.* **5**:646.

- Pan, J., Li, Z., Wang, Q., Yang, L., Yao, F., and Liu, W. (2020). An S-domain receptor-like kinase, OsESG1, regulates early crown root development and drought resistance in rice. *Plant Sci.* **290**:110318.
- Park, J., Kim, T.-H., Takahashi, Y., Schwab, R., Dressano, K., Stephan, A.B., Ceciliato, P.H.O., Ramirez, E., Garin, V., Huffaker, A., and Schroeder, J.I. (2019). Chemical genetic identification of a lectin receptor kinase that transduces immune responses and interferes with abscisic acid signaling. *Plant J.* **98**:492–510.
- Pi, L., Yin, Z., Duan, W., Wang, N., Zhang, Y., Wang, J., and Dou, D. (2022). A G-type lectin receptor-like kinase regulates the perception of oomycete apoplastic expansin-like proteins. *J. Integr. Plant Biol.* **64**:183–201.
- Qi, T., Seong, K., Thomazella, D.P.T., Kim, J.R., Pham, J., Seo, E., Cho, M.-J., Schultink, A., and Staskawicz, B.J. (2018). NRG1 functions downstream of EDS1 to regulate TIR-NLR-mediated plant immunity in *Nicotiana benthamiana*. *Proc. Natl. Acad. Sci. USA* **115**:E10979–E10987.
- Qiao, Z., Yates, T.B., Shrestha, H.K., Engle, N.L., Flanagan, A., Morrell-Falvey, J.L., Sun, Y., Tschaplinski, T.J., Abraham, P.E., Labbé, J., et al. (2021). Towards engineering ectomycorrhization into switchgrass bioenergy crops via a lectin receptor-like kinase. *Plant Biotechnol. J.* **19**:2454–2468.
- Robatzek, S., and Wirthmueller, L. (2013). Mapping FLS2 function to structure: LRRs, kinase and its working bits. *Protoplasma* **250**:671–681.
- Roux, M., Schwessinger, B., Albrecht, C., Chinchilla, D., Jones, A., Holton, N., Malinovsky, F.G., Tör, M., de Vries, S., and Zipfel, C. (2011). The *Arabidopsis* leucine-rich repeat receptor-like kinases BAK1/SERK3 and BKK1/SERK4 are required for innate immunity to hemibiotrophic and biotrophic pathogens. *Plant Cell* **23**:2440–2455.
- Schellenberger, R., Crouzet, J., Nickzad, A., Shu, L.-J., Kutschera, A., Gerster, T., Borie, N., Dawid, C., Cloutier, M., Villaume, S., et al. (2021). Bacterial rhamnolipids and their 3-hydroxyalkanoate precursors activate *Arabidopsis* innate immunity through two independent mechanisms. *Proc. Natl. Acad. Sci. USA* **118**:e2101366118.
- Schnepf, V., Vlot, A.C., Kugler, K., and Hükelhoven, R. (2018). Barley susceptibility factor RACB modulates transcript levels of signalling protein genes in compatible interaction with *Blumeria graminis* f.sp. *hordei*. *Mol. Plant Pathol.* **19**:393–404.
- Senthil-Kumar, M., and Mysore, K.S. (2014). Tobacco rattle virus-based virus-induced gene silencing in *Nicotiana benthamiana*. *Nat. Protoc.* **9**:1549–1562.
- Sermons, S.M., and Balint-Kurti, P.J. (2018). Large Scale Field Inoculation and Scoring of Maize Southern LeafBlight and Other Maize Foliar Fungal Diseases. *Bio. Protoc.* **8**:e2745.
- Shang, L., Li, X., He, H., Yuan, Q., Song, Y., Wei, Z., Lin, H., Hu, M., Zhao, F., Zhang, C., et al. (2022). A super pan-genomic landscape of rice. *Cell Res.* **32**:878–896.
- Shrestha, H., Yao, T., Qiao, Z., Muchero, W., Hettich, R.L., Chen, J.-G., and Abraham, P.E. (2023). Lectin receptor-like kinase signaling during engineered *Ectomycorrhiza* colonization. *Cells* **12**:1082.
- Smith, S.M., Steinau, M., Trick, H.N., and Hulbert, S.H. (2010). Recombinant Rp1 genes confer necrotic or nonspecific resistance phenotypes. *Mol. Genet. Genomics.* **283**:591–602.
- Sun, X.-L., Yu, Q.-Y., Tang, L.-L., Ji, W., Bai, X., Cai, H., Liu, X.-F., Ding, X.-D., and Zhu, Y.-M. (2013a). GsSRK, a G-type lectin S-receptor-like serine/threonine protein kinase, is a positive regulator of plant tolerance to salt stress. *J. Plant Physiol.* **170**:505–515.
- Sun, Y., Li, L., Macho, A.P., Han, Z., Hu, Z., Zipfel, C., Zhou, J.-M., and Chai, J. (2013b). Structural basis for flg22-induced activation of the *Arabidopsis* FLS2-BAK1 immune complex. *Science* **342**:624–628.
- Sun, Y., Ma, S., Liu, X., and Wang, G.-F. (2023). The maize ZmVPS23-like protein relocates the nucleotide-binding leucine-rich repeat protein Rp1-D21 to endosomes and suppresses the defense response. *Plant Cell* **35**:2369–2390.
- Takayama, S., Shimosato, H., Shiba, H., Funato, M., Che, F.S., Watanabe, M., Iwano, M., and Isogai, A. (2001). Direct ligand-receptor complex interaction controls *Brassica* self-incompatibility. *Nature* **413**:534–538.
- Tamura, K., Stecher, G., and Kumar, S. (2021). MEGA11: Molecular Evolutionary Genetics Analysis Version 11. *Mol. Biol. Evol.* **38**:3022–3027.
- Tian, T., Liu, Y., Yan, H., You, Q., Yi, X., Du, Z., Xu, W., and Su, Z. (2017). agriGO v2.0: a GO analysis toolkit for the agricultural community, 2017 update. *Nucleic Acids Res.* **45**:W122–W129.
- Tobias, C.M., and Nasrallah, J.B. (1996). An S-locus-related gene in *Arabidopsis* encodes a functional kinase and produces two classes of transcripts. *Plant J.* **10**:523–531.
- Tobias, C.M., Howlett, B., and Nasrallah, J.B. (1992). An *Arabidopsis* thaliana gene with sequence similarity to the S-locus receptor kinase of *Brassica oleracea*: sequence and expression. *Plant Physiol.* **99**:284–290.
- Trontin, C., Kiani, S., Corwin, J.A., Hématy, K., Yansouni, J., Kliebenstein, D.J., and Loudet, O. (2014). A pair of receptor-like kinases is responsible for natural variation in shoot growth response to mannitol treatment in *Arabidopsis thaliana*. *Plant J.* **78**:121–133.
- Vaid, N., Macovei, A., and Tuteja, N. (2013). Knights in action: lectin receptor-like kinases in plant development and stress responses. *Mol. Plant* **6**:1405–1418.
- van der Burgh, A.M., Postma, J., Robatzek, S., and Joosten, M.H.A.J. (2019). Kinase activity of SOBIR1 and BAK1 is required for immune signalling. *Mol. Plant Pathol.* **20**:410–422.
- Walker, J.C., and Zhang, R. (1990). Relationship of a putative receptor protein kinase from maize to the S-locus glycoproteins of *Brassica*. *Nature* **345**:743–746.
- Wang, X., and Duan, C. (2020). Reorganization of maize disease and causal agent names and discussion on their standardized translation of Chinese names. *Sci Agric Sin Advance*. Access published 2020.
- Wang, Z., Cheng, J., Fan, A., Zhao, J., Yu, Z., Li, Y., Zhang, H., Xiao, J., Muhammad, F., Wang, H., et al. (2018). LecRK-V, an L-type lectin receptor kinase in *Haynaldia villosa*, plays positive role in resistance to wheat powdery mildew. *Plant Biotechnol. J.* **16**:50–62.
- Wang, Y., Subedi, S., de Vries, H., Doornenbal, P., Vels, A., Hensel, G., Kumlehn, J., Johnston, P.A., Qi, X., Bliou, I., et al. (2019). Orthologous receptor kinases quantitatively affect the host status of barley to leaf rust fungi. *Nat. Plants* **5**:1129–1135.
- Wang, H., Hou, J., Ye, P., Hu, L., Huang, J., Dai, Z., Zhang, B., Dai, S., Que, J., Min, H., et al. (2021). A teosinte-derived allele of a MYB transcription repressor confers multiple disease resistance in maize. *Mol. Plant* **14**:1846–1863.
- Wang, M.-Y., Chen, J.-B., Wu, R., Guo, H.-L., Chen, Y., Li, Z.-J., Wei, L.-Y., Liu, C., He, S.-F., Du, M.-D., et al. (2023a). The plant immune receptor SNC1 monitors helper NLRs targeted by a bacterial effector. *Cell Host Microbe* **31**:1792–1803.e7.
- Wang, R., Li, C., Jia, Z., Su, Y., Ai, Y., Li, Q., Guo, X., Tao, Z., Lin, F., and Liang, Y. (2023b). Reversible phosphorylation of a lectin-receptor-like kinase controls xylem immunity. *Cell Host Microbe* **31**:2051–2066.e7.
- Waterhouse, A.M., Procter, J.B., Martin, D.M.A., Clamp, M., and Barton, G.J. (2009). Jalview Version 2--a multiple sequence alignment editor and analysis workbench. *Bioinformatics* **25**:1189–1191.

- Yang, S., and Hua, J. (2004). A haplotype-specific Resistance gene regulated by BONZAI1 mediates temperature-dependent growth control in Arabidopsis. *Plant Cell* **16**:1060–1071.
- Yang, Q., Balint-Kurti, P., and Xu, M. (2017a). Quantitative Disease Resistance: Dissection and Adoption in Maize. *Mol. Plant* **10**:402–413.
- Yang, Q., He, Y., Kabahuma, M., Chaya, T., Kelly, A., Borrego, E., Bian, Y., El Kasm, F., Yang, L., Teixeira, P., et al. (2017b). A gene encoding maize caffeoyl-CoA O-methyltransferase confers quantitative resistance to multiple pathogens. *Nat. Genet.* **49**:1364–1372.
- Yang, P., Praz, C., Li, B., Singla, J., Robert, C.A.M., Kessel, B., Scheuermann, D., Lüthi, L., Ouzunova, M., Erb, M., et al. (2019). Fungal resistance mediated by maize wall-associated kinase ZmWAK-RLK1 correlates with reduced benzoxazinoid content. *New Phytol.* **221**:976–987.
- Yin, Z., Liu, J., and Dou, D. (2024). RLKdb: A comprehensively curated database of plant receptor-like kinase families. *Mol. Plant* **17**:513–515.
- Zhong, T., Zhu, M., Zhang, Q., Zhang, Y., Deng, S., Guo, C., Xu, L., Liu, T., Li, Y., Bi, Y., et al. (2024). The ZmWAKL-ZmWIK-ZmBLK1-ZmRBOH4 module provides quantitative resistance to gray leaf spot in maize. *Nat. Genet.* **56**:315–326.
- Zhou, J.-M., and Zhang, Y. (2020). Plant Immunity: Danger Perception and Signaling. *Cell* **181**:978–989.
- Zhou, H., Mazzulla, M.J., Kaufman, J.D., Stahl, S.J., Wingfield, P.T., Rubin, J.S., Bottaro, D.P., and Byrd, R.A. (1998). The solution structure of the N-terminal domain of hepatocyte growth factor reveals a potential heparin-binding site. *Structure* **6**:109–116.
- Zhou, D., Godinez-Vidal, D., He, J., Teixeira, M., Guo, J., Wei, L., Van Norman, J.M., and Kaloshian, I. (2023). A G-type lectin receptor kinase negatively regulates Arabidopsis immunity against root-knot nematodes. *Plant Physiol.* **193**:721–735.
- Zhu, W., Zaidem, M., Van de Weyer, A.-L., Gutaker, R.M., Chae, E., Kim, S.-T., Bemm, F., Li, L., Todesco, M., Schwab, R., et al. (2018). Modulation of ACD6 dependent hyperimmunity by natural alleles of an Arabidopsis thaliana NLR resistance gene. *PLoS Genet.* **14**:e1007628.
- Zhu, M., Tong, L., Xu, M., and Zhong, T. (2021). Genetic dissection of maize disease resistance and its applications in molecular breeding. *Mol. Breed.* **41**:32.
- Zipfel, C. (2014). Plant pattern-recognition receptors. *Trends Immunol.* **35**:345–351.
- Zou, X., Qin, Z., Zhang, C., Liu, B., Liu, J., Zhang, C., Lin, C., Li, H., and Zhao, T. (2015). Over-expression of an S-domain receptor-like kinase extracellular domain improves panicle architecture and grain yield in rice. *J. Exp. Bot.* **66**:7197–7209.
- Zuo, W., Chao, Q., Zhang, N., Ye, J., Tan, G., Li, B., Xing, Y., Zhang, B., Liu, H., Fengler, K.A., et al. (2015). A maize wall-associated kinase confers quantitative resistance to head smut. *Nat. Genet.* **47**:151–157.